

Impact of Age and Obesity on Anthropometry

by

Zachary Forest Merrill

Bachelor of Science, University of Pittsburgh, 2013

Submitted to the Graduate Faculty of
Swanson School of Engineering in partial fulfillment
of the requirements for the degree of
Doctor of Philosophy

University of Pittsburgh

2019

UNIVERSITY OF PITTSBURGH
SWANSON SCHOOL OF ENGINEERING

This dissertation was presented

by

Zachary Forest Merrill

It was defended on

March 18, 2019

and approved by

Mark Redfern, Ph.D., Professor
Department of Bioengineering

April Chambers, Ph.D., Research Assistant Professor
Department of Bioengineering

Subashan Perera, Ph.D., Professor
Department of Medicine

Dissertation Director: Rakié Cham, Ph.D., Associate Professor
Department of Bioengineering

Copyright © by Zachary Forest Merrill

2019

Impact of Age and Obesity on Anthropometry

Zachary Forest Merrill, PhD

University of Pittsburgh, 2019

Current anthropometric models do not account for the variations of age, obesity, and individual body shape within the American working population. The goals of this dissertation are to determine the associations of age and body mass index (BMI) with commonly used anthropometric parameters, develop predictive regression models to accurately determine these parameters in individuals, and develop predictive regressions for body fat in adults. A data set of 280 working adults was collected, consisting of 88 skinfold and anthropometric measurements, along with a full body dual energy x-ray absorptiometry (DXA) scan. Body segment parameters (BSPs) including segment mass, center of mass, and radius of gyration, along with body composition, were determined from the analyses of these DXA scans.

Several significant effects of age, BMI, and individual body shape were found on body composition and the BSPs of interest. Specifically, the results showed significant changes in the center of mass and radius of gyration in large segments including the torso and thigh, with increasing age and obesity. When including individual body measurements to make predictive BSP models, the parameters of interest could be predicted with less than 5% root mean square error, and all of the predictions were more accurate than established anthropometric data sets, which had average errors of up to 60%. The body fat predictions improved upon previous statistical models by including age and BMI along with several skinfold and anthropometric measures. Body fat percentage was predicted with average errors of less than 10%, while established models result in errors of up to 33%.

In order to determine the importance of including representative BSP sets, static lifting and dynamic slipping sensitivity analyses were performed using various age, BMI, and anthropometric inputs. The static lifting task demonstrated variations of up to 12% in calculated L5/S1 compression force, based on the age and BMI inputs used, while the slipping task showed variations in hip joint forces and moments of up to 22% between individuals, highlighting the need for representative segment parameters.

Table of Contents

1.0 Introduction.....	1
1.1 Anthropometry Applications and Development.....	1
1.1.1 Anthropometry Applications	1
1.1.2 Development Methods	2
1.2 Goals and Specific Aims.....	5
2.0 Age and Body Mass Index Associations with Body Segment Parameters.....	7
2.1 Introduction	7
2.2 Methods	11
2.2.1 Participants and Settings.....	11
2.2.2 Statistical Analysis	14
2.3 Results.....	15
2.4 Discussion	26
3.0 Predictive Regression Modeling of Body Segment Parameters using Individual- Based Anthropometric Measurements	31
3.1 Introduction	31
3.2 Methods	33
3.2.1 Participants and Settings.....	33
3.2.2 Statistical Analysis	36
3.3 Results.....	37
3.3.1 Overview	37

3.3.2 Torso.....	38
3.3.3 Thigh	40
3.3.4 Shank.....	41
3.3.5 Upper Arm.....	43
3.3.6 Forearm.....	44
3.4 Discussion	46
3.4.1 Torso.....	47
3.4.2 Thigh	47
3.4.3 Shank.....	48
3.4.4 Upper Arm.....	49
3.4.5 Forearm.....	49
4.0 Impact of the Seated Height to Stature Ratio on Torso Segment Parameters.....	51
4.1 Introduction	51
4.2 Methods	53
4.2.1 Study Population	53
4.2.2 Statistical Analysis	56
4.3 Results.....	57
4.4 Discussion	61
5.0 Development and Validation of Body Fat Prediction Models in American Adults.....	67
5.1 Introduction	67
5.2 Methods	69
5.3 Results.....	73
5.4 Discussion	76
6.0 Discussion and Conclusions	81

6.1 Summary	81
6.2 Applications.....	84
6.2.1 Sensitivity Analyses	84
6.2.2 Body Fat Definition of Obesity	88
6.3 Conclusions	90
Bibliography	93

List of Tables

Table 1: Development of methods used to generate BSPs, including acquisition of source data and populations, along with advantages and disadvantages for each type.	8
Table 2: Female research participant characteristics	17
Table 3: Male research participant characteristics.....	17
Table 4: Descriptive statistics of female BSPs, stratified by age and BMI groups. Values are given as mean \pm standard deviation.	19
Table 5: Descriptive statistics of male BSPs, stratified by age and BMI groups. Values given as mean \pm sd.	20
Table 6: Parameters for females in each BMI category, within each age group.	21
Table 7: Parameters for males in each BMI category, within each age group.	22
Table 8: P, R^2 , and beta values for BMI and BMI ² for each segment parameter. Beta values are provided as estimate \pm standard error.	23
Table 9 (Females): P values for BMI, age, and BMI x age interaction terms, as well as nested P values for adding age and interaction terms. P ₁ represents the significance of adding age and age ² terms to the initial model only using BMI terms, and P ₂ represents the significance of adding the BMI x age interaction terms to the model only using BMI and age terms. ΔR^2_1 represents the increase in R^2 between the fitted models.....	24
Table 10 (Males): P values for BMI, age, and BMI x age interaction terms, as well as nested P values for adding age and interaction terms. P ₁ represents the significance of adding age and age ² terms to the initial model only using BMI terms, and P ₁ represents the significance of adding the BMI x age interaction terms to the model only using BMI and age terms. ΔR^2_1 represents the increase in R^2 between the fitted models.....	25
Table 11: Final regression equations for the full models using age, BMI, and all interactions. ..	27
Table 12: Sample torso parameter calculation for young and old (25 and 65 years, respectively), normal weight and morbidly obese male subjects, compared to the deLeva parameters. 29	
Table 13: Anthropometric measurements collected. All arm and leg measurements were performed on left and right sides.	35

Table 14: Torso regression results. Beta values provided for the intercepts and all remaining ($p < 0.10$) predictors following the elimination process.....	39
Table 15:Thigh regression results. Beta values provided for the intercepts and all remaining ($p < 0.10$) predictors following the elimination process.....	42
Table 16: Shank regression results. Beta values provided for the intercepts and all remaining ($p < 0.10$) predictors following the elimination process.	42
Table 17: Upper arm regression results. Beta values provided for the intercepts and all remaining ($p < 0.10$) predictors following the elimination process.....	43
Table 18: Forearm regression results. Beta values provided for the intercepts and all remaining ($p < 0.10$) predictors following the elimination process.	45
Table 19: R^2 values compared to old models (R^2_0) using only BMI and age terms.	45
Table 20: Root mean square error (RMSE) values for the model predictions normalized to the actual measured values in the testing subset, and percent differences between the predicted and actual values, and between deLeva predicted and actual values, given as mean (sd).....	46
Table 21: Descriptive statistics for the study population. Values are given as mean \pm sd.	56
Table 22: Regression results for females. Bolded values indicate $P < 0.05$	59
Table 23: Regression results for males. Bolded values indicate $P < 0.05$	60
Table 24: R^2 , ΔR^2 , F, and P values for the full regressions including age, BMI, and SHS terms for females (top) and males (bottom). R^2_I is for the initial model only using age and BMI terms, and R^2_F is for the full model also including the SHS terms. ΔR^2 is the additional variation explained by the model when adding the SHS, (SHS x Age), and (SHS x BMI) terms to the model only including the age and BMI terms. The nested F test represents the statistical significance in adding these three terms to the model at the same time. Bolded values indicate $P < 0.05$	61
Table 25: 3DSSPP sensitivity analysis results. The analysis was performed for females in the stoop lift position, with a 65 N downward force applied to each hand. Compression forces are provided in N.....	65
Table 26: Descriptive statistics for the study population. Values are shown as mean (sd).	70
Table 27: Anthropometric measures collected for body fat prediction.	72
Table 28: Descriptive statistics for the training and testing subsets. Values are shown as mean (sd).	73

Table 29: Average absolute percent errors for each prediction method. Values given as mean (sd). Errors calculated as the absolute difference between prediction methods and DXA measured values, divided by DXA measured values..... 76

Table 30: DXA derived obesity status compared to BMI, RFM, WHR, and Aim 4 predicted models. DXA obesity is determined from the actual values measured, while RFM and Aim 4 obesity is determined from the predictive models. DXA, RFM, and Aim 4 used body fat percentage cutoffs of 22.8% for men, and 33.9% for women. WHR uses obesity cutoffs of 0.85 for women, and 0.90 for men, while BMI uses a cutoff of 30.0 for men and women. 89

List of Figures

Figure 1: Example of a whole body DXA scan.	12
Figure 2: Segmental boundaries of interest: (a) forearm, (b) upper arm, (c) torso, (d) thigh, (e) shank.	14
Figure 3: Sample scatter plots for the torso segment parameters in females (left) and males (right). Lines plotted are the results of the initial linear regression analysis of BMI and BMI ² on the parameters of interest, and do not account for age.....	18
Figure 4: Sample DXA scan with torso delineation. The solid white lines separate the torso segment from the rest of the body. The thoracic torso segment is between the superior torso boundary and the dotted line. The lumbar segment is between the dotted and dashed lines, and the pelvis segment is the inferior section below the inferior dashed line. The full torso segment is between the superior torso boundary and the dashed line.....	54
Figure 5: Female model in the stoop lift position.	64
Figure 6: Root mean square error for the testing group for the newly developed prediction model, and the Hodgdon, Durnin, Jackson, and Woolcott models.....	75
Figure 7: Predicted body fat differences, shown as predicted body fat minus DXA measured body fat for each established prediction method. Error bars represent standard error. * indicates $p < 0.05$ compared to DXA measured values.	75
Figure 8: Left hip normalized extension moment outputs during unexpected slip and response for each individual input set. Positive moments represent extension, and negative moments represent flexion.....	86
Figure 9: Normalized peak hip reaction forces. Lines shown represent the minimum, average, and maximum model outputs for each measure, across all sets of anthropometric inputs.	87
Figure 10: Normalized peak hip reaction moments. Lines shown represent the minimum, average, and maximum model outputs for each measure, across all sets of anthropometric inputs.....	87

1.0 Introduction

1.1 Anthropometry Applications and Development

1.1.1 Anthropometry Applications

Body segment parameters (BSPs), which include the length, mass, center of mass (COM), and radius of gyration (R_G) of body parts, are used in a number of applications related to human factors and ergonomics, static and dynamic biomechanical modeling, and military and automobile operations. Applications utilizing BSP information, such as static and ergonomic modeling tools (Chaffin, Andersson, and Martin, 2006), and inverse dynamics applications (de Looze et al., 1992), have been proven to depend on accurate anthropometric inputs (Chaffin and Muzaffer, 1991; Desjardins et al., 1998; Pearsall and Costigan, 1999; Rao et al., 2006), highlighting the need for using representative, accurate segment parameter inputs.

Depending on how BSP data sets are derived, they can be optimized for different specific purposes, while being limited in their potential applications. For example, studies using dynamic analysis optimization (Chen et al., 2011; Hansen et al., 2014; Venture, Ayusawa, and Nakamura, 2009) are collected with predefined joint centers and segment end points that optimize the results for use in inverse dynamics calculations. The works of Chandler (1975), Dempster (1955), Hanavan (1964), McConville (1980), and Young (1983) have studied the mass distribution,

inertial properties, and space requirements of military personnel, while research by Reed and Ebert (2013) has observed body shape and surface modeling of seated operators, making these results directly applicable to military and automobile related applications.

Recent work performed by the University of Michigan Transportation Research Institute (UMTRI) has developed statistical models of body shapes, for military personnel (Reed and Ebert, 2013) and children (Park and Reed, 2015). These studies are particularly interesting because they account for overall body shape, which is particularly useful for inclusion in ergonomic modeling of lower back compressive forces, and the related injury risk, along with automobile design.

1.1.2 Development Methods

Previous work has approached the need for representative anthropometric sets by developing parameter sets for specific populations, such as the elderly (Chambers et al., 2010; Chambers et al., 2011), obese adults (Matrangola, 2008), children (Ganley and Powers, 2004; Park and Reed, 2015), and military personnel (Dempster, 1955; Hanavan, 1964; McConville et al., 1980; Reed and Ebert, 2013), however there are no available data sets which account for the specific *variations* in age, obesity, and individual body and segment shape in the American adult population.

Several methods for approximating BSPs have been developed and validated, including imaging, cadaver, static and dynamic analyses, and photogrammetric analysis. Some of the earliest attempts used cadaver studies (Chandler, 1975; Clauser et al., 1969; Dempster, 1955) in order to directly measure the masses and inertial properties of body segments. Cadaver methods

have the advantage of not relying on any density or mass distribution assumptions within each segment, however they do not allow for in vivo measurements. While some of the specific parameters resulting from the studies may be adjusted to utilize different endpoints (Hinrichs, 1990), the cadaver method of data collection does not easily allow for determination of segments using different endpoints or boundaries.

Geometric methods of determining BSPs, such as those done by Hanavan (1964), allow for individual anthropometric approximations based on individual measurements, combined with estimations for tissue density and mass distribution within segments. These methods have the advantage of producing individual level data sets from simple body measurements, however the parameters calculations are dependent on density and tissue distribution assumptions.

Similarly to the geometric methods, photogrammetric methods (Dumas, Cheze, and Verriest, 2007; McConville et al., 1980; Sanders et al., 2015; Young et al., 1983) rely on measurements within individuals, however this method uses measurements of frontal and sagittal plane images. Compared to the geometric method, the photogrammetric method allows for more measurements in each segment, with improved reliability, but similarly to the geometric method, this method depends on tissue density and mass distribution assumptions in order to calculate mass and inertial parameters.

Dynamic analysis optimization methods have the advantage of directly approximating the measures of interest, without depending on any density or mass distribution assumptions by simultaneously collecting motion capture and force plate data (Chen et al., 2011; Hansen et al., 2014; Venture, Ayusawa, and Nakamura, 2009). While this method leads to results that are directly applicable to inverse dynamics analyses, the results are also subject to errors related to reflective marker motion cause by soft tissue artefacts, and the predefined segment endpoints and

joint rotation center assumptions may limit the further applications. Finally, while methods such as cadaver and imaging methods can be used to predict parameters in individuals, the parameters collected by dynamic optimization are limited to the individuals from whom the data is collected, in addition to the requirements of time and computational effort.

Imaging methods (Chambers et al., 2011; deLeva, 1996; Ganley and Powers, 2004; Merrill, Chambers, and Cham, 2017; Merrill et al., 2018) have the advantages of collecting in vivo measurements, and directly measuring tissue density and masses. Additionally, the segments derived from imaging methods are not constrained by predefined segment boundaries or endpoints (Merrill et al., 2018), and can be altered depending on the desired applications. Unfortunately, imaging methods require expensive equipment for data collection and analysis, and in the case of computed tomography scanning, can expose study participants to high levels of radiation.

Dual energy x-ray absorptiometry (DXA) scanning has the advantage over other imaging methods of being a low radiation and relatively inexpensive method of collecting in vivo BSPs and body composition. Unlike geometric and photogrammetric methods, DXA scanning does not depend on any tissue density or mass distribution assumptions, and unlike dynamic analysis methods, DXA scans can be analyzed with various segment endpoints and boundaries, allowing for the same scan data to be applied for multiple applications, which may require differing segment definitions. Combined with the collection of individual anthropometric measurements, DXA scanning is ideal for determining individual anthropometry, and quantifying statistical effects of age, obesity, and body shape. The end result of this work includes validated BSP prediction models that can be used by others who do not have access to DXA scanning systems.

1.2 Goals and Specific Aims

The overall goals of this dissertation are to quantify the associations of age, BMI, and overall body shape with DXA scan derived segment parameters, and develop predictive models for segment parameters and body fat in individuals, using statistical regressions that include age, BMI, and individual anthropometric measurements. The specific aims and hypotheses are as follows:

- **Specific Aim 1: Quantify the impact of obesity and aging on normalized BSPs.**
 - Hypothesis H1.1: BMI will have a significant effect on normalized BSPs, particularly on those of large body segments such as the trunk and thigh.
 - Hypothesis H1.2: Age will have a significant effect on normalized BSPs when added to models already using BMI.
 - Hypothesis H1.3: Effects of BMI on normalized BSPs (H1.1) will increase with advancing age.
- **Specific Aim 2: Develop validated regression models to predict BSPs that include BMI.**
 - Hypothesis H2.1: By including age, gender and BMI as potential predictors along with other commonly used anthropometric variables, we will be able to predict BSPs with a root mean square error less than 5% of the mean.
 - Hypothesis H2.2: Predictions of BSPs in Hypothesis H2.1 will be more accurate than predictions derived from regression equations commonly used in the literature, both in development/training and validation samples.

- **Specific Aim 3: Define torso segment parameters for thoracic, lumbar, and pelvis segments, and quantify the impacts of age, BMI, and SHS ratio on these parameters.**
 - Hypothesis H3.1: Age and BMI terms will have significant associations with these parameters.
 - Hypothesis H3.2: Inclusion of the SHS ratio and its interactions with age and BMI will have significant effects on these parameters.
- **Specific Aim 4: Develop validated statistical models to predict body fat percentage in working adults.**
 - Hypothesis H4.1: By including age, BMI, and anthropometric measures in addition to skinfold measures, we will be able to predict total body fat percentage with a root mean square error of less than 10% of the mean.
 - Hypothesis H4.2: Body fat percentage predictions from Hypothesis 4.1 will be more accurate than the predictions of existing models.

2.0 Age and Body Mass Index Associations with Body Segment Parameters

2.1 Introduction

Body segment parameters (BSPs), including the length, mass, center of mass, and radius of gyration of body parts, are used in many ergonomic applications, including the design of tools, protective clothing, equipment and workstations (Chaffin, Andersson, and Martin 2006). BSPs are also necessary to develop biomechanical tools and models required to minimize the risk of musculoskeletal injuries while performing occupational activities such as lifting or resulting from slips, trips and falls accidents (Durkin and Dowling 2003; Hughes et al. 2004; M Kuczmarski, R Kuczmarski, and Najjar 2000; Matrangola et al. 2008). Examples of specific applications utilizing BSPs include the 3D Static Strength Prediction Model and inverse dynamics calculations (Chaffin and Muzaffer 1991). Such tools, which are used to calculate joint forces and moments during a specified task and to determine the fraction of the population capable of safely completing a task, require BSPs as input.

As shown in Table 1, currently available BSP datasets are typically predicted from data collected in cadaver studies (Chandler et al. 1975; Dempster 1955), imaging techniques (deLeva 1996), geometric modeling of the body (Hanavan, 1964; Pavol, Owings, and Grabiner 2002), inverse dynamics analyses (Hansen et al., 2014), static force plate analyses (Chen et al., 2011; Damavandi, Farahpour, and Allard, 2009), and photographic analysis (Jensen, 1978; Sanders et

al., 2015). Large differences in parameters have been found when these methods are compared (as large as 40%) (Pearsall and Costigan 1999).

Table 1: Development of methods used to generate BSPs, including acquisition of source data and populations, along with advantages and disadvantages for each type.

Method	Studies	Advantages	Disadvantages
Imaging	Chambers et al, 2011 de Leva, 1996 Merrill et al, 2018	<ul style="list-style-type: none"> • Allows for in vivo measurement • Exact tissue densities and masses may be calculated • Segment endpoints and boundaries can be adjusted depending on desired BSP application 	<ul style="list-style-type: none"> • Expensive equipment required for collection and analysis • Techniques such as CT or DXA will involve varying levels of radiation • Parameters are limited to the frontal plane
Cadaver	Chandler et al, 1975 Dempster, 1955	<ul style="list-style-type: none"> • Exact tissue densities and masses can be calculated 	<ul style="list-style-type: none"> • Does not allow for in vivo measurements
Geometric	Hanavan, 1964 Pavol, Owings, and Grabiner, 2002	<ul style="list-style-type: none"> • BSPs can be approximated from sets of simple in vivo anthropometric measurements 	<ul style="list-style-type: none"> • Relies on assumptions regarding tissue density and distribution within segments
Dynamic analysis	Chen et al., 2011 Hansen et al., 2014 Venture, Ayusawa, and Nakamura, 2009	<ul style="list-style-type: none"> • Allows for in vivo data collection, without any tissue density, volume, or distribution assumptions 	<ul style="list-style-type: none"> • Requires simultaneous motion capture and force plate data collection • Relies on accurate marker placement, and pre-defined segment endpoints
Photogrammetric analysis	Dumas, Cheze, and Verriest, 2007 Jensen, 1978 McConville et al., 1980 Sanders et al., 2015 Young et al., 1983	<ul style="list-style-type: none"> • Allows for in vivo collection with a camera • Parameters can be determined for frontal and sagittal planes 	<ul style="list-style-type: none"> • Relies on tissue density, volume, and shape assumptions

The elliptical method developed by Jensen (1978) is particularly interesting because it offers a noninvasive method of approximating segment parameters, by dividing each segment into a series of horizontal elliptical slices. The primary disadvantage to using this method is that it relies on assumptions regarding tissue density and elliptical slice volume, which can impact segment parameter calculations, especially in the torso (Wicke and Dumas, 2010), while other methods using imaging or cadavers directly measure segment masses used to determine the desired parameters.

Methods using inverse dynamics and force plate analyses (Chen et al., 2011; Damavandi, Farahpour, and Allard, 2009; Hansen et al., 2014) provide approaches to approximate segment parameters based on optimization equations, bypassing the need for tissue volume and density assumptions. These methods are noninvasive, similar to the elliptical methods (Jensen, 1978; Sanders et al., 2015), however they still do not directly measure masses within body segments, meaning that these results cannot be easily adapted to differing segment definitions, which are especially prevalent when defining torso parameters (Merrill et al., 2018).

BSPs are typically estimated using anthropometric models developed based on data collected from normal-weight young adults and do not account for variations in age, body shape, or obesity status present in a real-world working population (Durkin and Dowling 2003). While some studies have observed specific anthropometry sets for elderly (Chambers et al., 2011; Hoang and Mombaur, 2015) or obese (Matrangola et al., 2008) subsets of the population, they have not quantified the specific impacts of age and BMI on these parameters within the full adult population. With over 60% of the US adult population having a BMI classified as being above normal weight ($\text{BMI} \geq 25.0 \text{ kg m}^{-2}$), and nearly 35% having a BMI considered obese ($\text{BMI} \geq 30.0 \text{ kg m}^{-2}$) (Ogden et al., 2014), anthropometry sets derived from specific segment of the

population will not be able to accurately describe the changes in parameters for age and obesity status differences in the population as a whole. Thus, BSPs predicted based on methods developed in normal-weight young adults may not accurately represent the wide range of body mass index (BMI) and age across the working American population. In particular, estimates of BSPs using traditional predictive methods may be inaccurate for older adults, with the errors being functions of gender and mass distribution, and vary with the type of parameter of interest (Chambers et al. 2011). For example, large segments' parameters such as those of the torso and thigh segments in older adults, differences of 20-50% were reported between the deLeva predicted estimates and DXA derived calculations (Chambers et al. 2011).

Using BSPs that are not representative of the anthropometry of individuals in the workplace can lead to errors in the outputs of the static/dynamic modeling analyses (Chaffin and Muzaffer 1991). More specifically, inverse dynamics models, specifically those calculating L5/S1 joint loading and related injury risk, have been shown to be sensitive to parameter estimations such as center of mass position, joint rotation center location, length, and mass (F de Looze et al. 1992; M de Looze et al. 1992; Desjardins, Plamondon, and Gagnon 1998). Other dynamic analyses, such as those used for knee and hip kinetic calculations during gait produce varying results between different standard anthropometry sets in normal and overweight adults, with deviations as high as 60% (Pearsall and Costigan 1999; Rao et al. 2006). Such large differences in calculated values can greatly decrease the accuracy of predicted injury risk during specific tasks.

The objective of this study is to first determine if age and BMI have indeed a significant impact on the segment mass, center of mass and radius of gyration of the following major body segments: torso, thigh, shank, upper arm, and forearm. The analysis also considered the

possibility of nonlinear associations, differential age-BSP associations in those with lower and higher BMI, and differential BMI-BSP associations in different age groups.

2.2 Methods

2.2.1 Participants and Settings

A total of 280 working adults participated in this study. Participants were recruited according to gender, age, and BMI, in order to attempt to enroll equal numbers in four BMI categories (normal weight: $18.5 \leq \text{BMI} < 25.0$, overweight: $25.0 \leq \text{BMI} < 30.0$, obese: $30.0 \leq \text{BMI} < 40.0$, and morbidly obese $\text{BMI} \geq 40.0 \text{ kg m}^{-2}$) across three age groups ($21 \leq \text{age} < 40$), middle ($40 \leq \text{age} < 55$), and old ($55 \leq \text{age} < 70$).

After obtaining informed written consent, each participant had his or her height and mass recorded to confirm eligibility based on BMI. Female participants of child bearing age were then required to complete a pregnancy test, with a negative result being required for eligibility. A whole body DXA scan (Hologic QDR 1000/W, Bedford, MA, USA) of each participant was then collected using the same methods used in prior studies (Chambers et al. 2010; Chambers et al. 2011), with the participant lying supine as shown in Figure 1. The scanner was calibrated daily using a radiographic phantom, according to the manufacturer's instructions. These scanners have shown to be consistent in the short and long term for tissue densities between 0.5 and 3.3 g cm^{-3} (Hangartner, 2007).



Figure 1: Example of a whole body DXA scan.

DXA scan processing procedures consisted of each scan being split into each major body segment of interest (torso, upper arm, forearm, thigh, and shank), defined using bony landmarks and anatomically defined planes (Chambers et al. 2010), as shown in Figure 2. Each segment was then split into 3.9 cm tall slices, perpendicular to the long axes of the bones for the arms and legs, and horizontal for the torso, in a similar method as described by Ganley and Powers (2004). Pixel densities had assumed values of 2.5-3.0 g cm⁻³ for bone, 0.9 g cm⁻³ for fat, and 1.08 g cm⁻³ for lean tissue. The segment mass, center of mass (COM) and radius of gyration (R_G) were then calculated from the known slice heights and masses using a custom MATLAB script (Mathworks, Natick, MA, USA).

Making the same assumptions as Ganley and Powers (2004), the center of mass of each slice was assumed to be at its geometric center, and the segments were modeled as sets of point masses along their longitudinal axes. Each segment center of mass was calculated from the mass of each slice, and the distance from the proximal (superior for torso) border to the slice's geometric center, summed and divided by the total segment mass. The proximal moment of inertia for each segment was determined with the slice masses and distances from the proximal border, and the moment of inertia about the center of mass was calculated from the proximal moment of inertia, segment mass, and center of mass location using the parallel axis theorem. Finally, the radius of gyration was calculated as the square root of the moment of inertia about the center of mass, divided by the segment mass.

All reported data for the forearm, upper arm, thigh, and shank were analyzed on the participants' self-reported dominant side. Values for segment mass were reported as percent of the total body mass. COM locations were reported as percent of the segment length, where a higher value indicates that the COM is located further in the distal (inferior for the torso)

direction. The R_G values were also reported as percent of the segment length, with the R_G location being measured from the calculated COM.

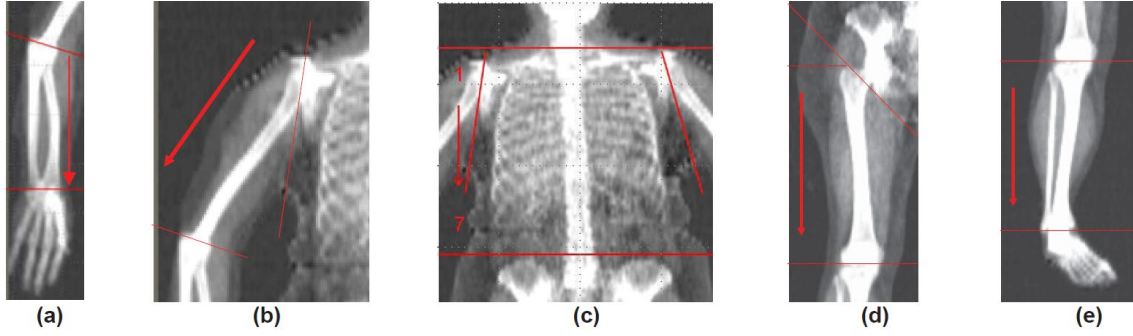


Figure 2: Segmental boundaries of interest: (a) forearm, (b) upper arm, (c) torso, (d) thigh, (e) shank.

2.2.2 Statistical Analysis

The statistical analyses were conducted using JMP Pro 12[®] (SAS Institute, Cary, NC, USA) with statistical significance set at $\alpha = 0.05$. All analyses were stratified by gender due to the significant differences between male and female participants. Parameters of interest were checked for normality, and log transformed as necessary before any further analysis.

For each BSP, least squares linear regression models were first fit using only BMI and BMI² as predictors in order to describe how BMI affected the parameters of interest, regardless of age. Next, to quantify the effect of age on top of the effect of BMI, age and age² were added to the initial BMI-only models. Finally, to examine whether age-BSP association varied with

BMI (or alternatively whether BMI-BSP association varied with age) the age x BMI, age² x BMI, age x BMI², and age² x BMI² interaction terms were added to the model. The coefficient of determination (R^2) was recorded for each model, and the increases (ΔR^2) were recorded for the model including the age and BMI terms, and the final model also including all of the interaction terms.

The nested models F-test was then used in order to determine the significance of adding set of predictors to the models. This test involved the relative decreases in the sum of squared errors in the final two sets of models, and allowed for the quantification of the significance of the increase in R^2 between models, again with statistical significance set at $\alpha = 0.05$.

2.3 Results

The study population consisted of 280 working adults (148 female) ages 21-70 (mean: 44.9 ± 13.4 years), as shown in Tables 2 (females) and 3 (males). Descriptive statistics for all segment parameters divided by gender, age, BMI, and combined age and BMI groups are provided in Tables 4 and Table 6 for females, and Tables 5 and 7 for and males. Figure 3 shows representative scatter plots for the torso parameters males and females, plotted with the regression line for the initial model only using BMI and BMI² as predictors.

The effect of both BMI and BMI² was found statistically significant for 7 and 6 BSPs (out of 15) in female and male participants, respectively (Table 8). More specifically, in female subjects, using only BMI and BMI² alone explained about 50% of the variability in the torso radius of gyration, 10-20% of the variability in the shank COM, shank radius of gyration,

forearm COM and upper arm radius of gyration, and 5-10% in the torso COM and thigh COM. Similarly, in male subjects, BMI and BMI² alone explained about 50% of the variability in torso radius of gyration, 30% of the variability in forearm mass, torso mass and COM, 10-20% of the variability in forearm radius of gyration, shank COM, and shank radius of gyration, and 5-10% of the variability in thigh COM and radius of gyration.

Adding age and age² to the model used only BMI revealed significant aging effects on 8 and 12 BSPs (out of 15) in female and male participants, respectively (P₁ values in Tables 9 and 10). In the female participants, aging effects were statistically significant for the torso segment (all 3 BSPs), the thigh mass and COM, the upper arm mass, the shank mass and COM. In male participants, aging effects were statistically significant for more BSPs than in female participants and included the torso segment (all 3 BSPs), the thigh mass and radius of gyration, upper arm mass and COM, the forearm COM and radius of gyration, and the shank (all 3 BSPs). More specifically, the age terms explained 5-10% beyond the variability explained by BMI terms alone in female torso and thigh mass, and torso radius of gyration, and 14% of the additional variability in torso COM. In males, the additional age terms explained 15-20% of the variability in thigh mass and radius of gyration, and torso COM, and 5-10% of the variability in torso radius of gyration, upper arm mass and radius of gyration, and forearm COM and radius of gyration.

Table 2: Female research participant characteristics

	All female	Age Group			BMI Group			
		Young	Middle	Old	Normal	Overweight	Obese	Morb. Obese
N	148	51	44	53	35	40	41	32
Mass (kg)								
Mean \pm SD	85.0 \pm 23.3	85.6 \pm 26.2	84.7 \pm 22.5	84.7 \pm 21.3	59.5 \pm 6.0	74.3 \pm 8.0	89.7 \pm 8.4	120.4 \pm 12.3
[min,max]	[41.9,149.6]	[41.9,149.6]	[50.4,135.0]	[51.8,140.5]	[41.9,69.0]	[57.8,90.9]	[72.6,112.9]	[100.2,149.6]
Stature (cm)								
Mean \pm SD	163.5 \pm 6.1	164.2 \pm 6.7	164.1 \pm 5.4	162.4 \pm 6.0	163.5 \pm 5.0	164.1 \pm 6.8	163.8 \pm 5.8	162.3 \pm 6.7
[min,max]	[149.5,177.9]	[150.6,177.9]	[149.5,174.6]	[151.5,175.4]	[150.6,176.2]	[149.5,174.6]	[152.7,175.4]	[151.5,177.9]
BMI (kg m ⁻²)								
Mean \pm SD	31.8 \pm 8.7	31.6 \pm 9.1	31.5 \pm 8.6	32.3 \pm 8.5	22.2 \pm 1.8	27.5 \pm 1.3	33.4 \pm 2.8	45.6 \pm 3.5
[min,max]	[18.5,57.6]	[18.5,53.3]	[19.6,49.8]	[21.0,57.6]	[18.5,24.9]	[25.2,29.9]	[30.0,40.0]	[41.3,57.6]
Age (y)								
Mean \pm SD	45.8 \pm 13.2	29.9 \pm 4.8	48.3 \pm 5.0	59.1 \pm 3.7	44.7 \pm 14.2	46.2 \pm 13.2	45.8 \pm 13.5	46.7 \pm 12.2
[min,max]	[21,70]	[21,39]	[40,54]	[55,70]	[21,70]	[24,66]	[21,63]	[23,68]

Table 3: Male research participant characteristics

	All male	Age Group			BMI Group			
		Young	Middle	Old	Normal	Overweight	Obese	Morb. Obese
N	132	45	49	38	33	41	38	20
Mass (kg)								
Mean \pm SD	94.9 \pm 24.6	93.2 \pm 23.4	94.2 \pm 26.2	97.9 \pm 24.0	69.3 \pm 7.7	84.7 \pm 7.4	106.5 \pm 12.9	136.3 \pm 13.5
[min,max]	[54.2,159.4]	[59.7,159.4]	[54.2,158.0]	[55.8,156.7]	[54.2,81.8]	[71.8,101.5]	[79.1,131.6]	[114.6,159.4]
Stature (cm)								
Mean \pm SD	176.5 \pm 6.9	177.4 \pm 5.7	175.5 \pm 7.4	176.8 \pm 7.5	175.3 \pm 6.5	175.7 \pm 6.6	178.3 \pm 7.9	176.7 \pm 5.6
[min,max]	[160.0,192.8]	[164.3,190.8]	[160.0,188.5]	[162.3,192.8]	[160.4,185.6]	[163.3,188.4]	[160.0,192.8]	[165.4,185.5]
BMI (kg m ⁻²)								
Mean \pm SD	30.4 \pm 7.2	29.6 \pm 7.1	30.4 \pm 7.7	31.2 \pm 6.9	22.5 \pm 1.7	27.4 \pm 1.2	33.4 \pm 3.0	43.6 \pm 2.5
[min,max]	[19.2,48.8]	[19.9,48.8]	[19.9,46.9]	[19.2,47.0]	[19.2,24.9]	[25.2,30.0]	[30.1,39.9]	[40.0,48.8]
Age (y)								
Mean \pm SD	44.0 \pm 13.6	27.7 \pm 5.4	46.9 \pm 4.7	59.5 \pm 3.8	40.4 \pm 14.1	44.2 \pm 14.8	44.6 \pm 12.5	48.2 \pm 11.9
[min,max]	[21,69]	[21,38]	[40,54]	[55,69]	[21,66]	[21,68]	[22,66]	[28,69]

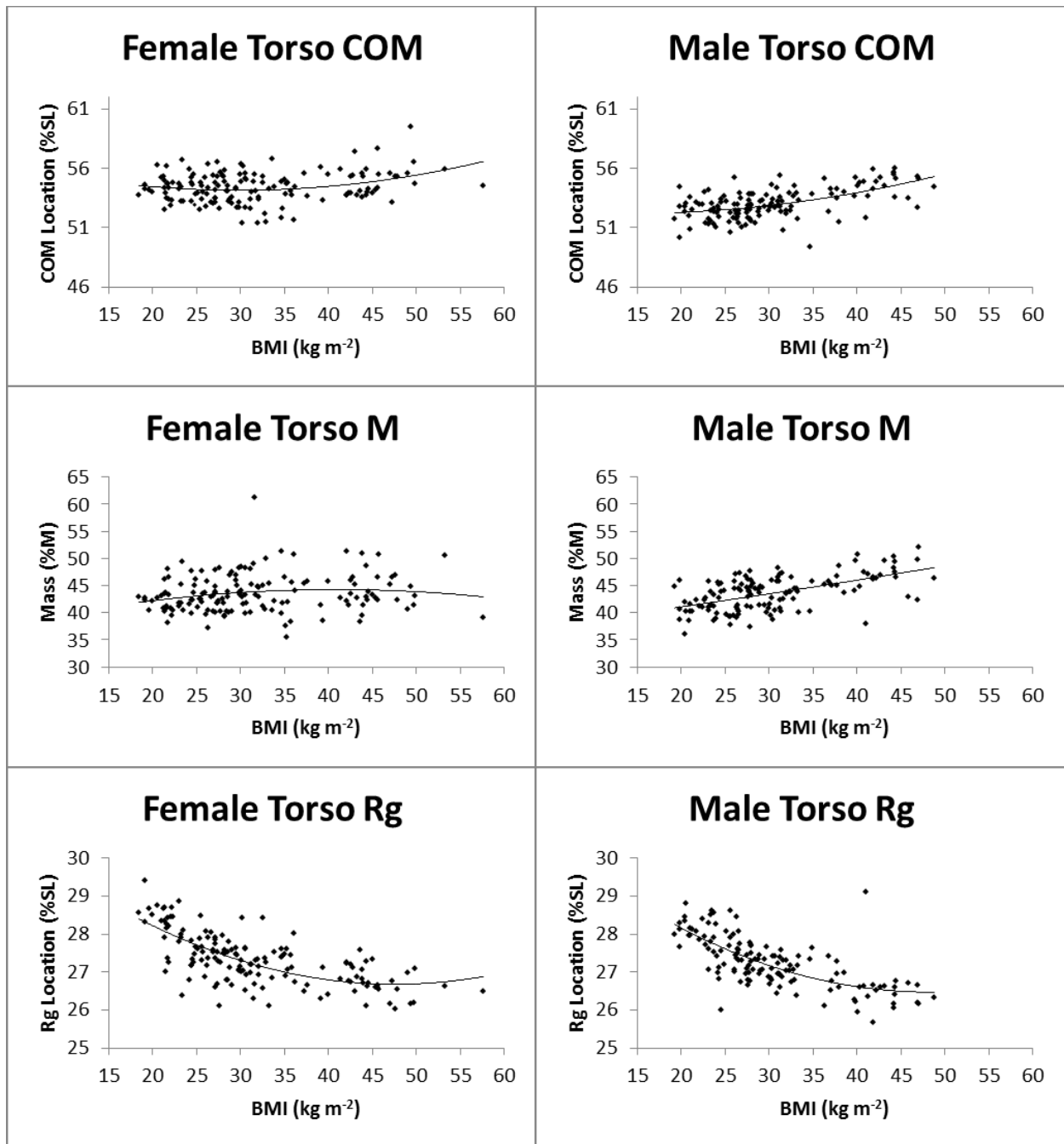


Figure 3: Sample scatter plots for the torso segment parameters in females (left) and males (right). Lines plotted are the results of the initial linear regression analysis of BMI and BMI² on the parameters of interest, and do not account for age.

Table 4: Descriptive statistics of female BSPs, stratified by age and BMI groups. Values are given as mean \pm standard deviation.

	All Female	Age Group			BMI Group			
		Young	Middle	Old	Normal	Overweight	Obese	Morb. Obese
N	148	51	44	53	35	40	41	32
Thigh COM (%SL)	45.8 \pm 1.6	45.7 \pm 1.5	45.4 \pm 1.7	46.2 \pm 1.6	45.7 \pm 1.5	45.7 \pm 1.4	45.5 \pm 1.7	46.5 \pm 1.9
Thigh Mass (%BW)	11.8 \pm 1.5	12.3 \pm 1.4	11.6 \pm 1.5	11.6 \pm 1.4	11.4 \pm 1.2	11.7 \pm 1.0	12.1 \pm 1.6	12.2 \pm 2.0
Thigh Rg (%SL)	25.7 \pm 0.5	25.6 \pm 0.4	25.7 \pm 0.5	25.8 \pm 0.6	25.7 \pm 0.6	25.8 \pm 0.5	25.6 \pm 0.4	25.7 \pm 0.5
Torso COM (%SL)	54.4 \pm 1.3	53.9 \pm 1.0	54.3 \pm 1.1	54.9 \pm 1.4	54.4 \pm 1.0	54.1 \pm 1.1	54.1 \pm 1.4	55.0 \pm 1.4
Torso Mass (%BW)	43.5 \pm 3.5	42.2 \pm 2.7	44.0 \pm 3.6	44.4 \pm 3.8	42.8 \pm 2.6	43.0 \pm 2.9	44.1 \pm 4.5	44.2 \pm 3.5
Torso Rg (%SL)	27.3 \pm 0.7	27.5 \pm 0.7	27.3 \pm 0.6	27.2 \pm 0.6	28.0 \pm 0.7	27.4 \pm 0.5	27.1 \pm 0.5	26.8 \pm 0.4
Upper Arm COM (%SL)	49.6 \pm 2.3	49.8 \pm 1.9	50.0 \pm 2.5	49.2 \pm 2.6	49.6 \pm 2.1	49.9 \pm 2.5	50.0 \pm 2.2	49.0 \pm 2.6
Upper Arm Mass (%BW)	3.5 \pm 0.4	3.4 \pm 0.4	3.5 \pm 0.5	3.6 \pm 0.4	3.3 \pm 0.3	3.4 \pm 0.3	3.5 \pm 0.4	3.8 \pm 0.5
Upper Arm Rg (%SL)	25.4 \pm 0.9	25.4 \pm 0.9	25.3 \pm 1.0	25.4 \pm 0.8	25.3 \pm 0.7	25.2 \pm 0.9	25.2 \pm 0.9	25.9 \pm 0.9
Forearm COM (%SL)	41.3 \pm 1.4	41.4 \pm 1.0	41.0 \pm 1.3	41.5 \pm 1.7	41.7 \pm 0.9	41.6 \pm 0.9	41.4 \pm 1.1	40.7 \pm 2.2
Forearm Mass (%BW)	1.4 \pm 0.2	1.4 \pm 0.2	1.4 \pm 0.2	1.3 \pm 0.2	1.5 \pm 0.1	1.4 \pm 0.1	1.4 \pm 0.2	1.2 \pm 0.2
Forearm Rg (%SL)	26.7 \pm 0.5	26.6 \pm 0.5	26.6 \pm 0.4	26.7 \pm 0.6	26.9 \pm 0.5	26.6 \pm 0.3	26.6 \pm 0.5	26.6 \pm 0.7
Shank COM (%SL)	40.1 \pm 1.3	40.4 \pm 1.1	40.0 \pm 1.2	39.9 \pm 1.6	41.1 \pm 0.9	40.3 \pm 0.9	39.6 \pm 1.0	39.5 \pm 1.8
Shank Mass (%BW)	4.2 \pm 0.6	4.4 \pm 0.5	4.1 \pm 0.7	4.1 \pm 0.5	4.5 \pm 0.4	4.3 \pm 0.5	4.1 \pm 0.6	3.9 \pm 0.7
Shank Rg (%SL)	26.1 \pm 0.6	26.1 \pm 0.5	26.2 \pm 0.5	26.2 \pm 0.6	26.4 \pm 0.5	26.1 \pm 0.5	26.0 \pm 0.5	26.0 \pm 0.6

The age x BMI interaction terms had minimal effects on the BSPs both in female and male participants (P_2 values in Tables 9 and 10). More specifically, these effects were statistically significant for only 3 out 15 BSPs in female and male groups, with additional variability ranging from 5-10% for torso, forearm, and shank COM in females, and upper arm mass, and forearm mass, COM, and radius of gyration in males.

Table 5: Descriptive statistics of male BSPs, stratified by age and BMI groups. Values given as mean \pm sd.

	All Male	Age Group			BMI Group			
		Young	Middle	Old	Normal	Overweight	Obese	Morb. Obese
N	132	45	49	38	33	41	38	20
Thigh COM (%SL)	46.5 \pm 1.9	46.2 \pm 1.2	46.6 \pm 2.5	46.9 \pm 1.5	47.2 \pm 1.5	47.0 \pm 1.4	45.8 \pm 2.5	45.9 \pm 1.4
Thigh Mass (%BW)	11.1 \pm 1.3	11.7 \pm 0.8	11.1 \pm 1.5	10.3 \pm 0.8	11.0 \pm 0.9	10.9 \pm 1.0	11.6 \pm 1.7	10.5 \pm 1.1
Thigh Rg (%SL)	25.3 \pm 0.4	25.2 \pm 0.4	25.2 \pm 0.4	25.5 \pm 0.4	25.4 \pm 0.4	25.3 \pm 0.4	25.2 \pm 0.4	25.2 \pm 0.5
Torso COM (%SL)	53.0 \pm 1.3	52.4 \pm 1.1	53.1 \pm 1.3	53.7 \pm 1.2	52.5 \pm 1.0	52.5 \pm 0.9	53.2 \pm 1.2	54.6 \pm 1.1
Torso Mass (%BW)	43.6 \pm 3.2	42.4 \pm 2.9	43.5 \pm 3.3	45.0 \pm 2.8	41.8 \pm 2.4	42.8 \pm 2.8	44.1 \pm 2.7	47.0 \pm 3.2
Torso Rg (%SL)	27.3 \pm 0.7	27.5 \pm 0.7	27.2 \pm 0.6	27.0 \pm 0.6	27.8 \pm 0.6	27.4 \pm 0.5	27.0 \pm 0.4	26.5 \pm 0.7
Upper Arm COM (%SL)	49.2 \pm 2.3	49.4 \pm 2.3	48.8 \pm 2.3	49.4 \pm 2.4	50.2 \pm 2.3	48.8 \pm 2.1	48.7 \pm 2.2	49.1 \pm 2.5
Upper Arm Mass (%BW)	3.8 \pm 0.4	3.9 \pm 0.5	3.9 \pm 0.3	3.7 \pm 0.4	3.7 \pm 0.3	3.9 \pm 0.3	4.0 \pm 0.5	3.8 \pm 0.4
Upper Arm Rg (%SL)	25.3 \pm 0.9	25.2 \pm 0.9	25.3 \pm 1.0	25.3 \pm 0.8	25.2 \pm 1.0	25.2 \pm 0.9	25.4 \pm 0.7	25.5 \pm 0.9
Forearm COM (%SL)	41.5 \pm 0.9	41.5 \pm 0.8	41.3 \pm 0.8	41.8 \pm 1.1	41.5 \pm 1.1	41.6 \pm 0.8	41.5 \pm 0.7	41.7 \pm 1.0
Forearm Mass (%BW)	1.6 \pm 0.3	1.7 \pm 0.2	1.6 \pm 0.4	1.6 \pm 0.2	1.8 \pm 0.2	1.7 \pm 0.1	1.6 \pm 0.2	1.4 \pm 0.2
Forearm Rg (%SL)	26.5 \pm 0.3	26.5 \pm 0.3	26.5 \pm 0.2	26.6 \pm 0.3	26.6 \pm 0.3	26.5 \pm 0.3	26.4 \pm 0.3	26.5 \pm 0.4
Shank COM (%SL)	40.7 \pm 0.9	40.7 \pm 0.9	40.5 \pm 1.0	41.0 \pm 0.9	41.3 \pm 0.8	40.7 \pm 0.8	40.4 \pm 0.9	40.5 \pm 1.1
Shank Mass (%BW)	4.1 \pm 0.5	4.2 \pm 0.5	4.0 \pm 0.5	4.0 \pm 0.4	4.4 \pm 0.4	4.1 \pm 0.3	3.9 \pm 0.4	3.5 \pm 0.4
Shank Rg (%SL)	26.4 \pm 0.6	26.4 \pm 0.6	26.4 \pm 0.5	26.4 \pm 0.6	26.8 \pm 0.5	26.4 \pm 0.5	26.2 \pm 0.5	26.2 \pm 0.5

Table 6: Parameters for females in each BMI category, within each age group.

FEMALE	Young				Middle				Old			
	NW	OW	OB	MO	NW	OW	OB	MO	NW	OW	OB	MO
N	13	13	13	12	10	13	13	8	12	14	15	12
Thigh COM (%SL)	45.7 ± 1.0	45.1 ± 1.3	45.8 ± 1.4	46.5 ± 2.0	45.8 ± 1.8	45.8 ± 1.5	44.3 ± 1.6	46.3 ± 1.6	45.7 ± 1.8	46.3 ± 1.1	46.2 ± 1.4	46.8 ± 2.1
Thigh Mass (%BW)	12.2 ± 1.1	11.9 ± 0.7	12.7 ± 1.4	12.6 ± 2.3	10.7 ± 0.9	11.6 ± 1.2	12.2 ± 1.5	11.9 ± 1.9	11.0 ± 1.0	11.6 ± 1.0	11.6 ± 1.6	11.9 ± 1.9
Thigh Rg (%SL)	25.6 ± 0.4	25.7 ± 0.2	25.5 ± 0.4	25.8 ± 0.6	25.7 ± 0.5	25.8 ± 0.4	25.5 ± 0.4	25.7 ± 0.6	25.7 ± 0.8	25.8 ± 0.6	25.7 ± 0.4	25.7 ± 0.5
Torso COM (%SL)	54.0 ± 0.8	53.7 ± 1.0	53.4 ± 1.3	54.5 ± 0.8	54.3 ± 1.0	54.1 ± 1.0	54.0 ± 1.4	55.0 ± 1.0	54.8 ± 1.2	54.6 ± 1.0	54.9 ± 1.4	55.5 ± 1.9
Torso Mass (%BW)	41.5 ± 1.5	42.3 ± 2.4	42.2 ± 3.6	42.7 ± 3.0	43.7 ± 3.0	43.6 ± 3.8	44.2 ± 3.9	44.9 ± 4.0	43.4 ± 2.8	43.1 ± 2.3	45.6 ± 5.4	45.3 ± 3.2
Torso Rg (%SL)	28.4 ± 0.5	27.6 ± 0.6	27.2 ± 0.2	26.9 ± 0.3	28.0 ± 0.6	27.3 ± 0.4	27.1 ± 0.6	26.6 ± 0.4	27.5 ± 0.7	27.4 ± 0.4	27.1 ± 0.7	26.7 ± 0.4
Upper Arm COM (%SL)	49.5 ± 2.2	50.1 ± 2.0	50.0 ± 1.5	49.3 ± 1.9	49.3 ± 2.3	50.2 ± 3.0	50.9 ± 2.3	49.1 ± 2.2	49.9 ± 2.0	49.4 ± 2.5	49.1 ± 2.5	48.5 ± 3.4
Upper Arm Mass (%BW)	3.2 ± 0.2	3.4 ± 0.3	3.4 ± 0.4	3.5 ± 0.5	3.3 ± 0.4	3.5 ± 0.4	3.4 ± 0.3	4.0 ± 0.6	3.3 ± 0.3	3.5 ± 0.4	3.6 ± 0.5	3.8 ± 0.3
Upper Arm Rg (%SL)	25.6 ± 0.8	25.0 ± 0.8	25.1 ± 0.9	26.1 ± 0.6	25.2 ± 0.8	24.9 ± 1.1	25.2 ± 1.0	26.2 ± 0.9	25.1 ± 0.6	25.7 ± 0.6	25.2 ± 0.9	25.5 ± 1.1
Forearm COM (%SL)	42.1 ± 1.3	41.1 ± 0.5	41.3 ± 0.8	41.3 ± 1.1	41.4 ± 0.5	41.2 ± 0.6	41.0 ± 1.1	40.4 ± 2.6	41.4 ± 0.5	42.4 ± 0.9	41.8 ± 1.3	40.3 ± 2.7
Forearm Mass (%BW)	1.5 ± 0.1	1.4 ± 0.1	1.4 ± 0.2	1.3 ± 0.2	1.5 ± 0.1	1.5 ± 0.1	1.4 ± 0.2	1.3 ± 0.2	1.5 ± 0.2	1.4 ± 0.1	1.3 ± 0.2	1.2 ± 0.3
Forearm Rg (%SL)	26.9 ± 0.7	26.5 ± 0.2	26.5 ± 0.3	26.6 ± 0.4	26.8 ± 0.3	26.6 ± 0.4	26.5 ± 0.3	26.6 ± 0.7	26.9 ± 0.4	26.7 ± 0.4	26.8 ± 0.6	26.5 ± 0.9
Shank COM (%SL)	41.5 ± 0.7	40.6 ± 0.9	39.8 ± 0.6	39.8 ± 1.3	40.9 ± 1.0	39.9 ± 0.8	39.6 ± 1.0	39.6 ± 1.6	40.7 ± 0.8	40.3 ± 0.9	39.6 ± 1.3	39.0 ± 2.4
Shank Mass (%BW)	4.8 ± 0.2	4.3 ± 0.4	4.3 ± 0.5	4.1 ± 0.6	4.3 ± 0.4	4.3 ± 0.6	4.0 ± 0.6	3.9 ± 1.1	4.3 ± 0.3	4.2 ± 0.3	4.0 ± 0.6	3.7 ± 0.5
Shank Rg (%SL)	26.3 ± 1.0	26.2 ± 1.3	26.0 ± 1.4	25.7 ± 2.0	26.2 ± 1.8	26.2 ± 1.5	26.0 ± 1.6	26.2 ± 1.6	26.8 ± 1.8	25.8 ± 1.1	26.1 ± 1.4	26.2 ± 2.1

Table 7: Parameters for males in each BMI category, within each age group.

MALE	Young				Middle				Old			
	NW	OW	OB	MO	NW	OW	OB	MO	NW	OW	OB	MO
N	13	13	13	6	14	14	14	7	6	14	11	7
Thigh COM (%SL)	47.1 ± 1.1	46.2 ± 1.0	45.8 ± 1.0	44.9 ± 0.9	47.2 ± 1.4	47.3 ± 1.3	45.5 ± 4.1	46.4 ± 1.6	47.4 ± 2.4	47.4 ± 1.5	46.4 ± 0.8	46.4 ± 1.1
Thigh Mass (%BW)	11.4 ± 0.6	11.8 ± 0.9	12.1 ± 0.6	11.4 ± 1.2	11.1 ± 0.6	10.6 ± 0.9	11.9 ± 2.4	10.2 ± 0.8	9.9 ± 1.1	10.4 ± 0.7	10.6 ± 0.8	10.0 ± 0.9
Thigh Rg (%SL)	25.4 ± 0.3	25.1 ± 0.2	25.0 ± 0.4	25.0 ± 0.5	25.3 ± 0.4	25.2 ± 0.4	25.1 ± 0.5	25.2 ± 0.5	25.8 ± 0.3	25.5 ± 0.5	25.4 ± 0.3	25.4 ± 0.4
Torso COM (%SL)	52.0 ± 0.9	52.4 ± 0.8	52.4 ± 1.2	53.5 ± 1.1	52.6 ± 0.8	52.2 ± 0.9	53.4 ± 1.0	54.9 ± 0.7	53.3 ± 0.9	52.9 ± 1.0	53.9 ± 0.9	55.1 ± 0.8
Torso Mass (%BW)	41.8 ± 1.9	41.9 ± 2.6	42.2 ± 2.7	45.2 ± 4.4	41.0 ± 2.7	43.1 ± 3.0	44.9 ± 2.5	46.9 ± 2.6	43.9 ± 1.9	43.4 ± 2.7	45.5 ± 1.3	48.5 ± 2.1
Torso Rg (%SL)	28.2 ± 0.4	27.6 ± 0.4	27.2 ± 0.3	26.9 ± 1.1	27.7 ± 0.5	27.4 ± 0.5	26.8 ± 0.5	26.5 ± 0.3	27.4 ± 0.9	27.2 ± 0.4	26.9 ± 0.3	26.3 ± 0.3
Upper Arm COM (%SL)	51.1 ± 2.1	49.0 ± 1.5	48.8 ± 2.3	48.2 ± 3.0	49.4 ± 2.4	48.8 ± 2.4	47.8 ± 1.9	49.2 ± 2.3	50.4 ± 2.4	48.6 ± 2.4	49.6 ± 2.4	49.9 ± 2.3
Upper Arm Mass (%BW)	3.6 ± 0.2	3.9 ± 0.2	4.2 ± 0.7	3.9 ± 0.2	3.8 ± 0.3	3.9 ± 0.3	4.0 ± 0.2	3.7 ± 0.4	3.4 ± 0.3	3.8 ± 0.4	3.7 ± 0.4	3.7 ± 0.4
Upper Arm Rg (%SL)	25.1 ± 1.0	25.3 ± 0.7	25.2 ± 0.9	25.5 ± 1.1	25.2 ± 0.9	25.0 ± 1.3	25.6 ± 0.6	25.8 ± 0.7	25.3 ± 1.1	25.2 ± 0.7	25.4 ± 0.7	25.1 ± 1.0
Forearm COM (%SL)	41.4 ± 0.6	41.1 ± 0.6	41.7 ± 0.6	41.9 ± 1.3	40.9 ± 0.9	41.7 ± 0.7	41.1 ± 0.5	41.9 ± 0.5	43.0 ± 1.0	41.9 ± 0.9	41.5 ± 1.0	41.4 ± 1.2
Forearm Mass (%BW)	1.8 ± 0.1	1.6 ± 0.1	1.7 ± 0.2	1.4 ± 0.1	1.8 ± 0.2	1.7 ± 0.1	1.6 ± 0.2	1.4 ± 0.2	1.7 ± 0.1	1.7 ± 0.1	1.6 ± 0.1	1.3 ± 0.2
Forearm Rg (%SL)	26.7 ± 0.2	26.5 ± 0.3	26.4 ± 0.3	26.6 ± 0.6	26.5 ± 0.2	26.6 ± 0.2	26.3 ± 0.2	26.4 ± 0.3	26.8 ± 0.3	26.5 ± 0.3	26.6 ± 0.3	26.6 ± 0.2
Shank COM (%SL)	41.5 ± 0.6	40.5 ± 0.6	40.5 ± 0.8	40.0 ± 0.9	40.9 ± 0.8	40.6 ± 1.1	40.0 ± 0.7	40.5 ± 1.2	41.8 ± 0.5	40.8 ± 0.7	40.8 ± 1.1	40.8 ± 1.2
Shank Mass (%BW)	4.6 ± 0.3	4.2 ± 0.3	4.1 ± 0.4	3.5 ± 0.1	4.3 ± 0.4	4.0 ± 0.3	3.8 ± 0.4	3.4 ± 0.4	4.3 ± 0.2	4.1 ± 0.3	3.9 ± 0.4	3.6 ± 0.5
Shank Rg (%SL)	26.8 ± 1.1	26.3 ± 1.0	26.0 ± 1.0	26.3 ± 0.6	26.8 ± 1.4	26.4 ± 1.3	26.0 ± 4.1	26.3 ± 1.6	26.6 ± 2.4	26.4 ± 1.5	26.6 ± 0.8	26.2 ± 1.1

Table 8: P, R², and beta values for BMI and BMI² for each segment parameter. Beta values are provided as estimate \pm standard error.

FEMALE	Thigh M			Thigh COM			Thigh Rg		
	P	R ²	$\beta \pm SE$	P	R ²	$\beta \pm SE$	P	R ²	$\beta \pm SE$
BMI	0.118		0.168 \pm 0.107	0.107		-0.189 \pm 0.117	0.086		-0.060 \pm 0.035
BMI ²	0.187	0.039	-0.002 \pm 0.002	0.052	0.065	0.003 \pm 0.002	0.076	0.022	0.001 \pm 0.0005
	Torso M			Torso COM			Torso Rg		
	P	R ²	$\beta \pm SE$	P	R ²	$\beta \pm SE$	P	R ²	$\beta \pm SE$
BMI	0.126		0.391 \pm 0.254	0.041		-0.186 \pm 0.090	<0.001		-0.194 \pm 0.036
BMI ²	0.188	0.032	-0.005 \pm 0.004	0.016	0.084	0.003 \pm 0.001	<0.001	0.492	0.002 \pm 0.001
	Upper Arm M			Upper Arm COM			Upper Arm Rg		
	P	R ²	$\beta \pm SE$	P	R ²	$\beta \pm SE$	P	R ²	$\beta \pm SE$
BMI	0.275		0.032 \pm 0.029	0.292		0.168 \pm 0.173	0.001		-0.174 \pm 0.062
BMI ²	0.649	0.146	-0.0001 \pm 0.0004	0.333	0.01	-0.003 \pm 0.002	0.006	0.132	0.003 \pm 0.001
	Forearm M			Forearm COM			Forearm Rg		
	P	R ²	$\beta \pm SE$	P	R ²	$\beta \pm SE$	P	R ²	$\beta \pm SE$
BMI	0.309		-0.012 \pm 0.012	0.002		0.236 \pm 0.093	0.741		-0.012 \pm 0.037
BMI ²	0.838	0.216	0.00004 \pm 0.0002	0.012	0.161	-0.004 \pm 0.001	0.962	0.056	-0.00003 \pm 0.001
	Shank M			Shank COM			Shank Rg		
	P	R ²	$\beta \pm SE$	P	R ²	$\beta \pm SE$	P	R ²	$\beta \pm SE$
BMI	0.066		-0.074 \pm 0.040	<0.001		-0.295 \pm 0.087	0.002		-0.124 \pm 0.039
BMI ²	0.197	0.126	0.001 \pm 0.001	0.008	0.208	0.003 \pm 0.001	0.005	0.105	0.002 \pm 0.001

MALE	Thigh M			Thigh COM			Thigh Rg		
	P	R ²	$\beta \pm SE$	P	R ²	$\beta \pm SE$	P	R ²	$\beta \pm SE$
BMI	0.049		0.243 \pm 0.131	0.076		-0.344 \pm 0.192	0.076		-0.077 \pm 0.043
BMI ²	0.065	0.037	-0.004 \pm 0.002	0.142	0.071	0.004 \pm 0.003	0.127	0.055	0.001 \pm 0.001
	Torso M			Torso COM			Torso Rg		
	P	R ²	$\beta \pm SE$	P	R ²	$\beta \pm SE$	P	R ²	$\beta \pm SE$
BMI	0.455		0.206 \pm 0.276	0.133		-0.663 \pm 0.110	<0.001		-0.204 \pm 0.050
BMI ²	0.875	0.322	0.001 \pm 0.004	0.546	0.325	0.002 \pm 0.002	0.006	0.506	0.002 \pm 0.001
	Upper Arm M			Upper Arm COM			Upper Arm Rg		
	P	R ²	$\beta \pm SE$	P	R ²	$\beta \pm SE$	P	R ²	$\beta \pm SE$
BMI	0.015		0.101 \pm 0.041	0.056		-0.462 \pm 0.239	0.519		-0.044 \pm 0.093
BMI ²	0.020	0.051	-0.001 \pm 0.001	0.084	0.045	0.006 \pm 0.004	0.635	0.019	0.001 \pm 0.001
	Forearm M			Forearm COM			Forearm Rg		
	P	R ²	$\beta \pm SE$	P	R ²	$\beta \pm SE$	P	R ²	$\beta \pm SE$
BMI	0.152		-0.041 \pm 0.029	0.754		-0.025 \pm 0.097	<0.001		-0.123 \pm 0.030
BMI ²	0.532	0.282	0.0003 \pm 0.0004	0.796	0.002	0.0005 \pm 0.001	<0.001	0.122	0.002 \pm 0.0005
	Shank M			Shank COM			Shank Rg		
	P	R ²	$\beta \pm SE$	P	R ²	$\beta \pm SE$	P	R ²	$\beta \pm SE$
BMI	0.236		-0.043 \pm 0.036	0.017		-0.222 \pm 0.092	<0.001		-0.241 \pm 0.053
BMI ²	0.994	0.454	-3.8E-6 \pm 0.001	0.049	0.126	0.003 \pm 0.001	<0.001	0.202	0.003 \pm 0.001

Table 9 (Females): P values for BMI, age, and BMI x age interaction terms, as well as nested P values for adding age and interaction terms. P_1 represents the significance of adding age and age² terms to the initial model only using BMI terms, and P_2 represents the significance of adding the BMI x age interaction terms to the model only using BMI and age terms. ΔR^2_1 represents the increase in R^2 between the fitted models.

FEMALE	Thigh M	Thigh COM	Thigh Rg	Torso M	Torso COM	Torso Rg	Upper Arm M	Upper Arm COM	Upper Arm Rg	Forearm M	Forearm COM	Forearm Rg	Shank M	Shank COM	Shank Rg
BMI	0.028	0.066	0.105	0.157	0.006	<0.001	0.202	0.359	0.007	0.355	0.025	0.438	0.078	<0.001	0.005
BMI ²	0.053	0.027	0.097	0.230	0.002	<0.001	0.489	0.293	0.002	0.907	0.009	0.626	0.218	0.001	0.015
Age	0.030	0.082	0.675	0.072	0.225	0.984	0.967	0.263	0.798	0.614	0.216	0.395	0.537	0.301	0.587
Age ²	0.070	0.053	0.831	0.152	0.068	0.622	0.773	0.229	0.724	0.458	0.210	0.297	0.737	0.199	0.490
Age x BMI	0.191	0.429	0.581	0.788	0.034	0.334	0.799	0.886	0.074	0.266	0.388	0.707	0.201	0.046	0.778
Age ² x BMI	0.139	0.327	0.576	0.961	0.017	0.465	0.792	0.986	0.095	0.188	0.659	0.541	0.213	0.029	0.726
Age x BMI ²	0.149	0.539	0.646	0.881	0.040	0.337	0.766	0.960	0.100	0.217	0.379	0.809	0.196	0.032	0.812
Age ² x BMI ²	0.103	0.420	0.641	0.957	0.020	0.454	0.775	0.912	0.129	0.153	0.065	0.626	0.206	0.019	0.755
P_1 (Age only)	<0.001	0.036	0.185	<0.001	<0.001	<0.001	0.009	0.423	0.905	0.167	0.645	0.171	0.015	0.014	0.382
ΔR^2_1	0.077	0.033	0.021	0.070	0.140	0.053	0.040	0.013	0.003	0.018	0.007	0.021	0.037	0.034	0.013
P_2 (Age x BMI)	0.106	0.446	0.942	0.212	0.038	0.245	0.726	0.505	0.089	0.121	0.007	0.309	0.786	0.020	0.970
ΔR^2_2	0.047	0.024	0.006	0.036	0.055	0.018	0.011	0.023	0.049	0.038	0.081	0.031	0.011	0.062	0.004

Table 10 (Males): P values for BMI, age, and BMI x age interaction terms, as well as nested P values for adding age and interaction terms. P_1 represents the significance of adding age and age² terms to the initial model only using BMI terms, and P_1 represents the significance of adding the BMI x age interaction terms to the model only using BMI and age terms. ΔR^2_1 represents the increase in R^2 between the fitted models.

MALE	Thigh M	Thigh COM	Thigh Rg	Torso M	Torso COM	Torso Rg	Upper Arm M	Upper Arm COM	Upper Arm Rg	Forearm M	Forearm COM	Forearm Rg	Shank M	Shank COM	Shank Rg
BMI	0.005	0.054	0.008	0.919	0.180	<0.001	0.004	0.056	0.645	0.369	0.221	<0.001	0.554	0.006	<0.001
BMI ²	0.005	0.113	0.017	0.489	0.032	0.017	0.007	0.082	0.536	0.841	0.198	<0.001	0.620	0.020	<0.001
Age	0.665	0.714	0.005	0.172	0.260	0.580	0.535	0.096	0.986	0.087	0.018	0.002	0.250	0.067	0.251
Age ²	0.707	0.533	<0.001	0.509	0.823	0.967	0.276	0.085	0.911	0.122	0.007	0.002	0.451	0.037	0.194
Age x BMI	0.417	0.515	0.016	0.073	0.945	0.958	0.221	0.718	0.721	0.037	0.080	0.007	0.730	0.322	0.799
Age ² x BMI	0.319	0.598	0.022	0.069	0.863	0.900	0.202	0.655	0.625	0.023	0.062	0.012	0.641	0.236	0.615
Age x BMI ²	0.570	0.441	0.013	0.114	0.885	0.892	0.389	0.751	0.662	0.071	0.086	0.006	0.812	0.372	0.883
Age ² x BMI ²	0.440	0.521	0.018	0.099	1.000	0.839	0.340	0.666	0.556	0.043	0.074	0.010	0.728	0.266	0.696
P_1 (Age only)	<0.001	0.176	<0.001	<0.001	<0.001	<0.001	0.001	0.013	0.959	0.530	0.002	<0.001	<0.001	0.003	0.034
ΔR^2_1	0.171	0.022	0.194	0.090	0.151	0.064	0.055	0.041	0.004	0.010	0.054	0.058	0.039	0.046	0.029
P_2 (Age x BMI)	0.229	0.748	0.119	0.063	0.125	0.913	0.031	0.414	0.277	0.025	0.002	0.035	0.704	0.287	0.447
ΔR^2_2	0.035	0.014	0.043	0.041	0.030	0.003	0.074	0.028	0.039	0.060	0.118	0.065	0.009	0.033	0.022

2.4 Discussion

Overall, the results indicate that there are significant associations of age, BMI, and the interactions between age and BMI with several body segment parameters in the working adult population. Additionally, the results revealed that age explains a significant amount of variability in BSPs above and beyond variability explained by BMI alone. The final regression models, show in Table 11, include the associations of BMI, age, and all of their interactions. While these equations have not been validated on an individual basis, they are still suitable for use in population based estimates.

The results of this study build upon previous preliminary analyses (Merrill, Chambers, and Cham, 2017) by observing the effects of age and BMI on the parameters of all major body segments, determining their associations with BMI terms, and more rigorously quantifying the improvement and statistical significance of adding age and the age x BMI interaction terms to the models. Further, this work improves upon other previous studies observing specific segment of the population such as the elderly and obese (Chambers et al., 2011; Hoang and Mombaur, 2015; Matrangola et al., 2008) by observing the changes in these parameters over wide ranges of age and obesity status, and quantifying the statistical associations of age and BMI on BSPs.

The results of the only BMI analysis indicated that BMI is significantly associated with certain BSPs in a non-linear manner in working adults. With the obesity epidemic in the labor force, such information could be used to provide more accurate insights into how BMI impacts the risk of musculoskeletal injuries in the workplace. For example, as anticipated, the fraction of the total body mass in the torso increases with BMI. Additionally, greater BMI is associated with a decreased torso radius of gyration in men and women, indicating that with greater BMI,

the mass of the torso becomes more concentrated in the area of the torso closer to the center of mass, as opposed to gaining mass throughout the torso. The results may impact internal back forces and moments in common site of injuries, e.g. L5/S1 disc. The results validate the need to take into account BMI when predicting BSPs, as up to 50% of the variability in some BSPs is explained by BMI. Thus, selecting a method to predict BSPs should be done with caution, by making sure the BMI characteristics of the population used to develop that specific method is comparable with the current population of interest.

Table 11: Final regression equations for the full models using age, BMI, and all interactions.

		Int	Age	Age ²	BMI	BMI ²	Age*BMI	Age*BMI ²	Age ² *BMI	Age ² *BMI ²
TORSO	COM	M	54.958	-0.189	3.41E-03	-0.0606	-2.29E-03	3.93E-03	1.25E-04	-1.16E-04
		F	27.625	1.722	-0.0215	1.652	-0.0233	-0.110	1.57E-03	1.39E-03
	M	M	122.438	-4.491	0.0543	-4.962	0.0680	0.270	-3.64E-03	-3.26E-03
		F	62.409	-0.629	1.31E-03	-1.341	0.0143	0.0415	-3.41E-04	-8.51E-05
	Rg	M	32.590	-0.025	-2.65E-04	-0.203	1.39E-03	-1.47E-03	5.84E-05	4.21E-05
		F	40.099	-0.326	2.56E-03	-0.728	9.82E-03	0.0206	-3.03E-04	-1.74E-04
THIGH	COM	M	30.846	0.911	-8.14E-03	1.367	-0.0264	-0.0742	1.34E-03	7.13E-04
		F	34.356	0.964	-0.0131	0.597	-4.59E-03	-0.0575	6.61E-04	7.96E-04
	M	M	-9.478	1.109	-0.0160	1.098	-0.0114	-0.0569	6.10E-04	8.31E-04
		F	30.926	-1.338	0.0167	-1.191	0.0209	0.0839	-1.37E-03	-1.06E-03
	Rg	M	44.214	-0.875	0.0101	-1.215	0.0192	0.0552	-8.76E-04	-6.22E-04
		F	30.801	-0.215	2.50E-03	-0.307	3.96E-03	0.0122	-1.51E-04	-1.38E-04
SHANK	COM	M	59.660	-0.970	0.0134	-0.988	0.0127	0.0526	-7.27E-04	-7.49E-04
		F	18.479	1.591	-0.0197	1.556	-0.0264	-0.105	1.67E-03	1.28E-03
	M	M	3.881	0.125	-2.09E-03	0.0509	-8.41E-04	-7.23E-03	7.60E-05	1.16E-04
		F	-4.092	0.479	-5.32E-03	0.599	-9.39E-03	-0.0319	4.77E-04	3.47E-04
	Rg	M	30.639	0.142	-3.12E-03	-0.274	4.66E-03	-7.89E-03	6.98E-05	1.85E-04
		F	30.395	-0.142	1.92E-03	-0.215	2.57E-03	6.92E-03	-8.64E-05	-9.63E-05
UPPER ARM	COM	M	73.803	-1.061	0.0142	-1.118	0.0132	0.0504	-6.77E-04	-7.40E-04
		F	29.220	0.551	-3.14E-03	0.934	-0.0109	-0.0157	8.00E-05	-2.17E-05
	M	M	-8.506	0.573	-7.02E-03	0.620	-6.63E-03	-0.0283	3.04E-04	3.51E-04
		F	1.411	0.060	-7.02E-04	0.128	-2.02E-03	-4.56E-03	7.90E-05	5.27E-05
	Rg	M	23.735	0.238	-3.98E-03	0.141	-2.91E-03	-0.0197	3.69E-04	3.21E-04
		F	53.169	-1.167	0.0124	-1.711	0.0244	0.0693	-9.43E-04	-7.22E-04
FOREARM	COM	M	68.923	-1.581	0.0207	-1.720	0.0273	0.0940	-1.41E-03	-1.19E-03
		F	64.695	-0.828	5.16E-03	-1.383	0.0204	0.0486	-7.35E-04	-2.78E-04
	M	M	-7.392	0.580	-7.47E-03	0.544	-7.19E-03	-0.0345	4.56E-04	4.47E-04
		F	3.400	-0.113	1.55E-03	-0.144	2.34E-03	8.41E-03	-1.38E-04	-1.11E-04
	Rg	M	43.570	-0.743	8.38E-03	-1.081	0.0170	0.0465	-7.30E-04	-5.17E-04
		F	26.009	0.162	-2.68E-03	8.09E-03	6.65E-04	-8.60E-03	8.21E-05	1.57E-04

The findings indicated that age also impacts BSPs, perhaps to a lesser extent than BMI. Thus, including age in a BSP predictive model would increase the accuracy of that model for few BSPs, especially the variables related to the torso (both men and women) and thigh (men). When applied to dynamic lifting or gait models, the age dependent differences in these larger segments will likely have significant impacts on hip moment and joint contact force calculations, and L5/S1 moment calculations. With the aging of the labor force, these age-related changes in BSPs are important to take into account.

Finally, findings suggested that the contributions of BMI and age are to a large extent additive as the impact of the age-BMI interactions are minimal. Including the interaction terms may be useful for the few parameters where the interaction terms are significant; however, for nearly all of the parameters, the interactions account for less than 10% additional explained variance.

When predicting segment parameters, it is necessary to include effects age and BMI in order to obtain most accurate parameters for a given individual. As an example of the variation in segment parameter calculation, Table 12 shows the torso segment parameters determined from the final age and BMI interaction models for males aged 25 and 65 years, with BMI of 20 and 40 kg m⁻². The current gold standard deLeva (1996) model-based parameters are also included for comparison. The calculated COM locations vary from 52.0 to 54.6 percent of the torso segment length, the mass fraction varies from 41.3 to 46.8 percent of the total body mass, and the radius of gyration calculations vary from 26.4 to 28.4 percent of the segment length. By comparison, the deLeva model is reasonably close for calculating segment mass, but underestimates the COM and radius of gyration values (44.9 and 19.1 percent, respectively), meaning that it may not account for variations in mass distribution within the segment. While the segment definitions

differ slightly, based on how the thighs are separated from the pelvis (Merrill et al., 2018), these differences do not affect the overall length of the torso segment, which could in turn impact the definition of parameters as percentages of segment length.

Table 12: Sample torso parameter calculation for young and old (25 and 65 years, respectively), normal weight and morbidly obese male subjects, compared to the deLeva parameters.

		Torso Parameter		
Age (y)	BMI (kg m ⁻²)	COM (%SL)	M (%BW)	Rg (%SL)
25	20	52.0	41.3	28.4
65	20	53.5	45.2	27.8
25	40	52.3	42.5	26.8
65	40	54.6	46.8	26.4
deLeva		44.9	43.5	19.1

Compared to the somewhat similar method of determining individual BSPs pioneered by Jensen (1978), and used in more recent studies (Sanders et al., 2015), this study used a similar technique involving creating transverse slices through each body segment. While Jensen's elliptical method used smaller slices, it also relied on assumed tissue density and slice volume functions, whereas this study could use the actual DXA derived masses of each segment. Additionally, Jensen's method involved the assumption that the segments had elliptical shaped cross sections of measured width and depth. The results of this study likely provide more representative segment parameters in individuals due to actually measuring the masses of each of the slices.

While methods using optimization algorithms to determine parameters from inverse dynamics (Hansen et al., 2014) and static positioning on force plates (Chen et al., 2011; Damavandi, Farahpour, and Allard, 2009) can estimate segment parameters in a non-invasive manner, they are somewhat limited to predefined anthropometric sets due to the placements of visual markers, and assumptions regarding these marker locations relative to anatomical axes and rotation centers. DXA scanning methods have the advantage of determining the masses of each pixel in the image, and determining segment boundaries based on specific anatomical landmarks, allowing more precise segment boundaries, which may be altered depending on the desired anthropometric data set and application (Merrill et al., 2018).

Some of the limitations for this study include the lack of information regarding fitness history and activity levels within the sample population, suggesting that these results may not be representative for athletic populations with disability. All of the DXA scans were collected with the participants lying supine, and thus a small amount of shifting in soft tissue likely occurred from the standing position. Despite these limitations, the findings of this study demonstrate that the wide variations in segment parameters are significantly associated with age and obesity status, indicating that predictive models including these factors are needed for calculating accurate parameters. Finally, regression equations only observe the associations of age and BMI with BSPs, and have not been validated to estimate BSPs for individuals or populations, therefore they should not be employed as predictive models.

3.0 Predictive Regression Modeling of Body Segment Parameters using Individual-Based Anthropometric Measurements

3.1 Introduction

Body segment parameters (BSPs), which include the length, mass, center of mass (COM), and radius of gyration (R_G) of body parts, are used in a number of applications related to human factors and ergonomics, as well as static and dynamic biomechanical modeling. Some of these specific ergonomic applications include the design of tools, protective clothing, equipment, and workstations (Chaffin, Andersson, and Martin, 2006) based on segment size and ranges of motion, while static models such as the 3D Static Strength Prediction Model are dependent on segment position, length, mass, and COM inputs (Chaffin and Muzaffer, 1991). Inverse dynamics models use these inputs in addition to the segment inertial properties and dynamic data in order to determine joint contact forces and moments, along with their related injury risk during a specified task.

The accuracy of the outputs of these biomechanics tools rely on the accuracy of the estimated segment parameters in the populations or individuals being studied. For example, inverse dynamics models, such as those related to lifting and related injury risk, have been shown to be sensitive to parameter estimations such as center of mass position, joint rotation center location, length, and mass (de Looze, F et al., 1992; de Looze M et al., 1992; Desjardins,

Plamondon, and Gagnon, 1998). Other dynamic analyses, such as those used for knee and hip kinematic calculations during gait, produce varying results between different standard anthropometry sets in normal and overweight adults, with deviations as high as 60% (Pearsall and Costigan, 1999; Rao et al., 2006). Such large differences in modeling outputs can negatively affect the ability to predict injury risk, and reflect the need for accurate segment parameter inputs.

In order to minimize these issues arising from modeling with non-representative BSPs, the sets of parameters used should be representative of the populations of interest or individuals being studied. Some of the previous parameter estimations have used regression equations from cadaver data (Chandler et al., 1975; Dempster, 1955), imaging techniques (de Leva, 1996), geometric modeling of the body (Pavol, Owings, and Grabiner 2002), inverse dynamics analyses (Hansen et al., 2014), static force plate analyses (Chen et al., 2011; Damavandi, Farahpour, and Allard, 2009), and photographic analysis (Jensen, 1978; Sanders et al., 2015). Comparisons between these methods have revealed that parameter predictions can vary by up to 40% (Durkin and Dowling, 2003). Additionally, weight loss (Matrangola et al., 2008) and age-related changes in body composition (Hughes et al., 2004; Kuczmarski, Kuczmarski, and Najjar, 2000) can also affect parameter determination. Because these methods separately study different population segments, such as normal weight young adults (de Leva, 1996), or older adults (Hughes et al., 2004; Kuczmarski, Kuczmarski, and Najjar, 2000; Pavol, Owings, and Grabiner, 2002), they do not account for the wide ranges of age, body mass index (BMI) within the current population.

Previous work has quantified the population level associations of age and BMI with BSPs in American adults (Merrill, et al., 2017). These associations were statistically and practically significant, and thus justify the need for BSP predictive data sets that reflect the effects of age

and obesity. Thus, the goal of this study is to develop statistical predictive models to accurately estimate BSPs using individual-based predictors. Previous research has indicated that there are significant relationships between age, BMI, and BSPs, so this study will build on these known relationships with the inclusion of individual anthropometric measurements. These statistical models will be developed and validated on a population of American adult workers covering wide age and obesity ranges, and the results will be used for calculating representative BSPs in individuals.

3.2 Methods

3.2.1 Participants and Settings

The study was approved by the University of Pittsburgh Institutional Review Board. A total of 280 working adults participated in this study. Recruitment was stratified by age group, BMI group and gender in an attempt to accurately represent the working population characteristics. More specifically, working men and women were recruited in equal numbers in four BMI categories (normal weight: $18.5 \leq \text{BMI} < 25.0$, overweight: $25.0 \leq \text{BMI} < 30.0$, obese: $30.0 \leq \text{BMI} < 40.0$, and morbidly obese $\text{BMI} \geq 40.0 \text{ kg m}^{-2}$) across three age groups ($21 \leq \text{age} < 40$), middle ($40 \leq \text{age} < 55$), and old ($55 \leq \text{age} < 70$).

After obtaining written informed consent, each participant had his or her height and mass recorded in order to confirm eligibility based on BMI. Female participants of child bearing age

were then required to complete a pregnancy test, with a negative result being required for eligibility. Next, approximately 60 anthropometric measurements were collected (Table 13), including segment lengths, widths, depths, and circumferences. All of the arm and leg measurements were collected for the dominant and non-dominant sides. A whole body DXA scan (Hologic QDR 1000/W, Bedford, MA, USA) of each participant was then collected using the same methods used and described in prior studies (Chambers et al., 2010), with the participant lying supine (Figure 1).

The analysis consisted of each scan being split into each major body segment of interest (torso, left and right upper arm, forearm, thigh, and shank), defined using bony landmarks and anatomically defined planes (Chambers et al., 2010), as shown in Figure 2. Each segment was then split into 3.9 cm tall slices, perpendicular to the long axes of the bones for the arms and legs, and horizontal for the torso, in a similar method as described by Ganley and Powers (2004). Pixel densities had assumed values of 2.5-3.0 g cm⁻³ for bone, 0.9 g cm⁻³ for fat, and 1.08 g cm⁻³ for lean tissue. The segment mass, center of mass (COM) and radius of gyration (R_G) were then calculated from the known slice heights and masses using a custom MATLAB script (Mathworks, Natick, MA, USA).

All reported data for the forearm, upper arm, thigh, and shank were analyzed on the participants' self-reported dominant side. Values for segment mass were reported as percent of the total body mass. COM locations were reported as percent of the segment length, where a higher value indicates that the COM is located further in the distal (inferior for the torso) direction. The R_G values were also reported as percent of the segment length, with the R_G location being measured from the calculated COM.

Table 13: Anthropometric measurements collected. All arm and leg measurements were performed on left and right sides.

Anthropometric variable	Definition
Waist circumference	Circumference at the umbilicus
Hip circumference	Around largest part of the hip
Upper thigh circumference	Around proximal thigh
Mid-thigh circumference	Around point midway between proximal border of patella and inguinal crease
Lower thigh circumference	Around thigh 1 cm above proximal border of patella
Knee circumference	Around medial and lateral femoral epicondyles
Calf circumference	Around largest part of calf
Ankle circumference	Around medial and lateral malleoli
Upper arm circumference	Around midpoint between acromion and olecranon processes
Elbow circumference	Around medial and lateral humeral epicondyles
Lower arm circumference	Around midpoint between lateral humeral epicondyle and ulnar styloid process
Wrist circumference	Around radial and ulnar styloid processes
Hand thickness	Thickness at center of palm
Elbow width	Distance between medial and lateral humeral epicondyles
Wrist width	Between radial and ulnar styloid processes
Knee width	Between medial and lateral epicondyles
Ankle width	Between medial and lateral malleoli
Upper arm length	Lateral humeral epicondyle to acromion
Lower arm length	Ulnar styloid process to lateral humeral epicondyle
Thigh length	Greater trochanter to knee joint center
Shank length	Knee joint center to lateral malleolus
Inter-ASIS distance	Between left and right ASIS
Shoulder level trunk width	Width at shoulder joint center level
Breast level trunk width	Width at nipple level
Mid-breast level trunk width	Width at level midway between nipple and L3-L4
L3-L4 level trunk width	Width at L3-L4 level
Shoulder level trunk depth	Depth at shoulder joint center level
Breast level trunk depth	Depth at nipple level
Mid-breast level trunk depth	Depth at level midway between nipple and L3-L4
L3-L4 level trunk depth	Depth at L3-L4 level
Shoulder level axis depth	Depth from the shoulder joint center/greater trochanter plane to the back at shoulder joint center level
Breast level axis depth	Depth from the shoulder joint center/greater trochanter plane to the back at nipple level
Mid-breast level axis depth	Depth from the shoulder joint center/greater trochanter plane to the back at level midway between nipple level and L3-L4
L3-L4 level axis depth	Depth from the shoulder joint center/greater trochanter plane to the back at L3-L4
C7 height	Distance from ground to C7
Shoulder height	Distance from ground to shoulder joint center
ASIS height	Distance from ground to ASIS
Hip height	Distance from ground to greater trochanter

3.2.2 Statistical Analysis

All fifteen segment parameters of interest (mass, COM, and R_G for the torso, thigh, shank, upper arm, and forearm) were separated by gender and checked for normality, then log transformed as necessary before any further analysis. The full data set of 280 participants was randomly split into two subgroups: the training set, which contained 200 participants, and the testing set, which contained the remaining 80. A multiple regression analysis was performed on the torso, thigh, shank, upper arm, and forearm segment parameters in the training subset with a backward elimination strategy for variable selection and stratified by gender. The initial models contained age, BMI, age and BMI interaction terms, waist, hip, and neck circumferences, and all relevant physical measures taken of the body segment of interest. While not direct measurement of all segments, the waist, hip, and neck circumferences were included to all initial models due to their relationship with overall body shape and mass distribution. For each model, genders were analyzed separately. In each step of the analysis, the predictor with the largest P-value was removed, and the analysis was repeated. This process of removing the least significant predictor and repeating the analysis continued until the p-values for all predictors were below 0.10. All analyses were performed in JMP Pro 12 (SAS Institute, Cary, NC, USA).

Once the training set models were finalized, they were applied to the anthropometric measures in the testing set, so that the predicted and actual segment (in-vivo DXA-based) parameters could be compared in the testing set, and used as a method of validating the models. Within the testing set, the actual and predicted values were compared by calculating the absolute percent error, as well as the root mean square error (RMSE). Additionally, the actual testing set

values were compared to a commonly used segment parameter prediction method (deLeva, 1996).

3.3 Results

3.3.1 Overview

The final study sample consisted of 280 working adults (148 female) ages 21-70 (mean: 44.9 ± 13.4 years). A number of significant effects were found from the anthropometric measurements on the segment parameters of interest in women and men (Tables 14-18), with all but one of the models showing improvement over the prediction method using only age, BMI, and interaction terms (Table 19). While not all of the models employed the additional anthropometric measures, the majority retained age, BMI, or interaction terms. The majority of the average prediction errors and normalized RMSE values were within 5% of the actual DXA-based values in the testing subset, while the parameter predictions based on the deLeva (1996) regressions demonstrated higher errors, in some cases up to 60% of the actual measured values (Table 20).

3.3.2 Torso

The initial torso models included the following variables as potential predictors of the torso BSPs (COM, mass and radius of gyration): age, BMI, their squared and interaction terms in addition to waist, hip, and neck circumference, torso widths, depths, and axis depths (Table 13), and the inter-ASIS distance. The backward elimination regression analyses identified a number of age- and BMI- related terms among the statistically significant factors, but also various anthropometric predictors (Table 14). When including all the predictor variables identified by the backward elimination regression analyses as being significantly associated with the torso BSPs, the final regression model explained an average 51% and 74% of the variability in the torso BSPs in female and male participants included in the training set, respectively. Including the anthropometric factors explained an additional 13 to 50% of the variability in the torso BSPs above and beyond that explained by the age- and BMI- related terms alone (Table 19). Most importantly, when the final regression models were used to predict the torso BSPs in the testing set, the normalized RMSE values were less than 5%, and the percent prediction errors (relative to the actual in-vivo DXA-based BSPs) were 3% or less. In contrast, the percent prediction errors of the deLeva method ranged between 6% (torso mass) to 34% (torso radius of gyration) (Table 20).

Table 14: Torso regression results. Beta values provided for the intercepts and all remaining ($p < 0.10$) predictors following the elimination process.

TORSO											Circumference		Width Level				Depth Level				Inter-ASIS
		Int	Age	Age^2	BMI	BMI^2	Age^3BMI	Age^3BMI^2	Age^3^3BMI	Age^3^3BMI^2	Neck	Hip	Shoulder	Breast	Mid breast	L3/L4	Shoulder	Breast	Mid breast	L3/L4	
COM	M	57.325	-0.0445	3.09E-04	-0.203	1.56E-03	--	4.64E-05	--	--	-0.119	--	--	-0.145	0.213	--	-0.149	--	--	0.102	0.105
	F	62.442	--	-2.11E-03	-0.614	9.03E-03	--	--	1.66E-04	2.52E-06	--	0.0567	-0.105	--	--	--	--	-0.143	--	--	0.099
M	M	120.217	-3.831	0.0458	-5.333	0.0842	0.261	-4.16E-03	-3.11E-03	5.02E-05	--	-0.127	--	--	--	--	-0.536	--	1.050	-0.336	0.266
	F	37.495	--	--	-1.274	9.10E-03	--	--	--	--	--	--	--	0.261	--	--	-0.295	0.767	--	0.445	--
Rg	M	39.743	-0.417	3.28E-03	-0.546	5.38E-03	0.0177	-1.22E-04	-1.09E-04	--	--	0.0261	--	--	--	-0.103	0.167	-0.0946	-0.0497	--	--
	F	33.183	-0.0967	--	-0.347	4.72E-03	5.66E-03	-7.65E-05	--	--	--	--	0.0821	--	-0.0483	--	--	--	--	-0.0712	--

3.3.3 Thigh

The thigh models initially included neck, waist, hip, knee, and three thigh circumferences, taken at the upper, middle, and lower thigh levels (Table 13), as well as knee width and thigh length. Almost all of the models retained at least one of the age or BMI terms, and all included at least one of the thigh circumference measurements (Table 15). For thigh COM, upper and lower thigh circumferences were both significant predictors, and both genders had ΔR^2 values over 0.2 (Table 19). Both genders also had similar ΔR^2 values for R_G predictions, however the female model retained almost all of the age, BMI, and interaction terms, while the male model was solely based on circumference measurements.

When applied to the testing subset, the thigh COM and R_G models had normalized RMSE values below 5%, while the mass RMSE was much higher, at 11.6% (Table 20). The thigh R_G mean error was comparable to the torso prediction errors, at about 1.1%, however the COM and mass predictions were slightly higher, at 3.8 and 7.0%, respectively. All three of the actual thigh parameters had errors of 16-38% when compared to the deLeva prediction methods (Table 20).

3.3.4 Shank

The shank prediction models started with neck, waist, hip, knee, calf, and ankle circumferences, as well as knee and ankle widths, and shank length. With the exception of shank COM in males, all of the other parameter predictions included at least one BMI term and calf circumference. In both genders, hip and calf circumferences were included in the final mass models, while waist, knee, and calf circumferences were used in the R_G models.

All of the models other than COM in males showed R^2 increases of over 0.2, with final R^2 values over 0.85 for mass in both genders (Table 19). The predictive power of the anthropometric model for shank COM in males showed a negligible increase of 0.004 over the previous model using only age and BMI terms. This model only included hip circumference and ankle width, but none of the age terms, or any of the other terms generally associated with obesity, such as BMI or waist circumference (Table 16). When applied to the testing sets, the COM and R_G predictions were especially accurate, with RMSE under 2.5%, and average errors of all three shank parameters under 5% (Table 20). Compared to the deLeva predicted parameters, the testing set parameters had higher error predictions, especially for R_G predictions, with average error of over 60%.

Table 15:Thigh regression results. Beta values provided for the intercepts and all remaining (p < 0.10) predictors following the elimination process.

THIGH											Circumference						
		Int	Age	Age^2	BMI	BMI^2	Age*BMI	Age*BMI^2	Age^2*BMI	Age^2*BMI^2	Neck	Waist	Hip	Upper thigh	Mid thigh	Lower thigh	Knee
COM	M	58.572	-0.438	5.32E-03	-0.264	--	0.0145	--	-1.76E-04	--	-0.107	--	--	--	--	0.227	--
	F	51.351	-0.172	2.08E-03	--	1.24E-03	--	--	--	--	0.111	--	-0.0947	-0.0894	--	0.186	--
M	M	11.882	--	-1.63E-04	--	--	--	--	--	--	-0.136	-0.0248	--	0.120	--	--	--
	F	32.272	-1.346	0.0148	-1.955	0.0262	0.0865	-1.29E-03	-9.63E-04	1.45E-05	-0.129	--	--	0.116	0.115	--	0.0927
Rg	M	24.421	--	--	--	--	--	--	--	--	0.05	--	-0.0194	-0.0331	-0.0374	--	0.129
	F	29.22	-0.196	0.00213	-0.129	--	0.0061	--	-6.63E-05	--	--	--	--	--	-0.056	--	0.0972

Table 16: Shank regression results. Beta values provided for the intercepts and all remaining (p < 0.10) predictors following the elimination process.

SHANK											Circumference					Ankle Width	
		Int	Age	Age^2	BMI	BMI^2	Age*BMI	Age*BMI^2	Age^2*BMI	Age^2*BMI^2	Shank Length	Waist	Hip	Knee	Calf		Ankle
COM	M	39.703	--	--	--	--	--	--	--	--	--	--	-0.0341	--	--	--	0.603
	F	46.963	--	-1.87E-03	-0.553	6.75E-03	--	--	1.20E-04	-1.78E-06	-0.110	--	--	-0.238	0.121	0.480	--
M	M	3.663	--	-8.45E-05	-0.168	1.00E-03	--	--	--	8.81E-08	--	--	-0.0127	--	0.146	--	--
	F	3.333	-0.0234	--	-0.217	1.32E-03	7.27E-04	--	--	--	--	--	-9.64E-03	--	0.153	0.0508	--
Rg	M	32.393	--	-2.19E-03	-0.281	4.82E-03	--	--	1.32E-04	-1.87E-06	0.0372	-0.0132	--	0.0905	-0.183	--	0.170
	F	26.146	--	--	--	4.59E-04	--	--	--	--	--	-0.0111	--	0.0406	-0.150	0.196	--

3.3.5 Upper Arm

In addition to the age and BMI terms, the upper arm models started with waist, hip, neck, upper arm, and elbow circumferences, and elbow width. The final model for predicting mass in females had an R^2 value of about 0.5 (Table 19), however all of the other models had R^2 of under 0.25. Even though the variance explained by the models approximately doubled for R_G in males and COM in females, the overall values still remained under 15%. The models for mass and R_G in males, and mass and COM in females all included waist and elbow circumferences (Table 17).

Table 17: Upper arm regression results. Beta values provided for the intercepts and all remaining ($p < 0.10$) predictors following the elimination process.

Upper Arm												Circumference			
		Int	Age	Age^2	BMI	BMI^2	Age*BMI	Age*BMI^2	Age**BMI	Age**BMI^2	Upper arm Length	Waist	Hip	Elbow	Upper Arm
COM	M	58.27	-0.229	2.50E-03	--	--	--	--	--	--	--	--	--	--	-0.124
	F	46.182	--	--	--	--	--	--	--	--	--	-0.0575	--	0.337	--
M	M	-6.28	0.365	-4.02E-03	0.249	--	-0.0121	--	--	1.33E-04	--	-0.0176	--	0.153	--
	F	2.432	-0.0243	1.07E-04	-0.0346	--	7.55E-04	--	--	--	0.0376	9.97E-03	-0.027	0.0411	0.0527
Rg	M	20.405	--	--	-0.122	--	--	--	--	--	--	0.0268	--	0.208	--
	F	35.337	-0.385	4.60E-03	-0.418	3.14E-03	0.0120	--	-1.43E-04	--	--	--	--	--	--

The final model for predicting R_G in females is notable because it did not improve over the previous model, which included all of the age, BMI, quadratic, and interaction terms. None of the anthropometric terms were significant in the final model, so the final R^2 ended up slightly less than the previous model because the non-significant age, BMI, and interaction terms were removed during the backwards elimination process. While the total variance explained by the

model was under 20% for R_G for both genders, the RMSE was under 4% when applied to the testing set, with an average error of less than 3% (Table 20). The upper arm COM prediction also had RMSE of less than 5%, while the mass prediction had a higher RMSE of about 10%. The errors compared to the deLeva predictions were again higher, ranging from approximately 17% for COM location, to almost 40% for R_G .

3.3.6 Forearm

The initial model for the forearm included the age and BMI terms along with waist, hip, neck, forearm, elbow, and wrist circumferences, wrist and elbow widths, and forearm length. All of the final models included at least one of the age or BMI terms, and all except for mass in females included wrist circumference (Table 18). While the mass predictions had the highest R^2 values, they also larger prediction errors in the testing set, with normalized RMSE of about 9%, and average errors over 7% (Table 20). COM and R_G predictions were more accurate when applied to the testing set, with RMSE under 2.5%, and average errors under 2%. Compared to the deLeva parameter predictions, the forearm mass prediction error was slightly higher than the anthropometric model errors, at a little over 11%, however the average error in R_G calculation is nearly 60%.

Table 18: Forearm regression results. Beta values provided for the intercepts and all remaining ($p < 0.10$) predictors following the elimination process.

Forearm												Circumference				
		Int	Age	Age^2	BMI	BMI^2	Age*BMI	Age*BMI^2	Age^2*BMI	Age^2*BMI^2	Forearm Length	Waist	Hip	Elbow	Forearm	Wrist
COM	M	41.396	-0.0259	1.11E-03	--	3.03E-03	--	6.88E-05	--	--	-0.168	--	--	-0.203	--	0.521
	F	48.113	-0.282	--	-0.529	8.05E-03	0.0177	-2.59E-04	--	--	--	--	-0.377	-0.221	--	0.690
M	M	-11.193	0.748	-9.58E-03	0.735	-0.010	-0.0441	6.09E-04	5.66E-04	-7.82E-06	--	-8.26E-03	-0.0145	--	0.0430	0.0897
	F	1.042	--	--	-0.03	3.35E-04	--	--	--	--	0.0214	-3.91E-03	-8.44E-03	0.0460	0.0243	--
Rg	M	28.227	-0.0397	4.48E-04	-0.0913	1.40E-03	--	--	--	--	--	--	--	--	-0.0994	0.169
	F	24.706	--	--	-0.0409	--	--	--	--	--	--	0.0160	--	--	-0.144	0.307

Table 19: R^2 values compared to old models (R^2_0) using only BMI and age terms.

Female	Torso COM	Torso Mass	Torso Rg	Thigh COM	Thigh Mass	Thigh Rg	Shank COM	Shank Mass	Shank Rg	Arm COM	Arm Mass	Arm Rg	Forearm COM	Forearm Mass	Forearm Rg
R^2	0.509	0.633	0.677	0.358	0.663	0.242	0.505	0.861	0.441	0.099	0.503	0.181	0.375	0.672	0.320
R^2_0	0.279	0.138	0.563	0.122	0.163	0.049	0.304	0.174	0.122	0.046	0.197	0.184	0.249	0.272	0.108
ΔR^2	0.230	0.495	0.114	0.236	0.500	0.193	0.201	0.687	0.319	0.053	0.306	-0.003	0.126	0.400	0.212
Male	Torso COM	Torso Mass	Torso Rg	Thigh COM	Thigh Mass	Thigh Rg	Shank COM	Shank Mass	Shank Rg	Arm COM	Arm Mass	Arm Rg	Forearm COM	Forearm Mass	Forearm Rg
R^2	0.635	0.660	0.739	0.387	0.558	0.570	0.209	0.853	0.622	0.131	0.218	0.133	0.338	0.446	0.400
R^2_0	0.506	0.453	0.573	0.107	0.440	0.292	0.205	0.502	0.253	0.114	0.180	0.062	0.174	0.352	0.245
ΔR^2	0.129	0.207	0.166	0.280	0.118	0.278	0.004	0.351	0.369	0.017	0.038	0.071	0.164	0.094	0.155

Table 20: Root mean square error (RMSE) values for the model predictions normalized to the actual measured values in the testing subset, and percent differences between the predicted and actual values, and between deLeva predicted and actual values, given as mean (sd).

	Torso			Thigh			Shank			Arm			Forearm		
	COM	Mass	Rg	COM	Mass	Rg	COM	Mass	Rg	COM	Mass	Rg	COM	Mass	Rg
RMSE	1.675	5.241	1.596	4.812	10.951	1.665	2.408	5.681	1.468	4.623	10.032	3.374	2.122	9.030	1.432
Diff (predicted)	1.34 (1.04)	4.35 (3.24)	1.25 (1.00)	3.01 (5.26)	6.17 (6.12)	1.23 (1.12)	1.98 (1.37)	4.46 (3.88)	1.15 (0.91)	3.63 (2.90)	7.48 (6.34)	2.68 (2.05)	1.57 (1.38)	6.81 (5.78)	0.88 (1.06)
Diff (deLeva)	19.65 (4.62)	6.36 (4.51)	33.94 (4.28)	16.85 (5.23)	27.09 (13.34)	38.78 (2.29)	9.66 (3.02)	15.02 (12.45)	62.81 (1.85)	16.83 (5.57)	26.22 (7.39)	39.67 (2.62)	9.84 (2.44)	11.60 (12.64)	59.82 (5.33)

3.4 Discussion

The new prediction models including individual anthropometric measures in addition to age and BMI terms have increased the accuracy over previous methods only considering gender (deLeva, 1996). These improvements in accuracy are particularly notable in the torso and thigh segments. The results show that the inclusion of the neck, waist, and hip circumferences are important to include along with BMI for all segment parameter predictions because they provide further insight into how mass is generally distributed throughout the body.

3.4.1 Torso

The torso parameter predictions in females, particularly COM and R_G , retained several of the age and BMI terms as being significant, while also each including 3-4 torso width and depth measurements. While all of the final R^2 values for the female torso predictions are above 0.5, the increases are especially notable for mass and COM predictions (Table 19), indicating that changes in these parameters are highly dependent on the torso geometry of the individual. The increase in variance explained for the torso R_G is smaller than the other two parameters, indicating that the differences among individuals is mostly explained by age and BMI, with a smaller portion being dependent on torso measurements.

Because the males had higher initial R^2 values, and lower ΔR^2 values compared to the females, the results indicate that while the final prediction models for males explain the majority of the variation, the models are largely controlled by the age and BMI factors, with anthropometric measurements playing a smaller role in parameter prediction. For all three of the male torso models, shoulder level depth was a highly significant factor ($p < 0.01$), meaning that the volume of the top of the torso, independent of tissue composition (lean or adipose), plays an important role in predicting these parameters.

3.4.2 Thigh

In females, the models for thigh COM and R_G retained most of the age and BMI predictors as being significant, meaning that while individual thigh anthropometry explains most

of the variation in thigh mass ($\Delta R^2 = 0.49$), age and obesity status explain the distribution of mass within this thigh. In males, most of the age and BMI factors are significant in COM prediction, while thigh mass and R_G predictions are almost entirely dependent on circumference measurements. The thigh R_G prediction in males is entirely dependent on circumference measurements (neck, hip, knee, and upper and mid-thigh), and does not include any of the initial age or BMI predictors, indicating that this parameter is only dependent on the shape of the individual, and independent of age or obesity status.

3.4.3 Shank

With the exception of shank COM prediction in males, all of the prediction models included calf circumference. The calf circumference measurement is notable because it is defined as the largest measurement around the calf, as opposed to other measurements, which are defined relative to anatomical landmarks. The calf circumference is a highly significant predictor ($p < 0.001$) for shank mass in both genders because it is proportional to the maximum cross section of the shank, instead of being in a predefined location. Similarly to the thigh R_G in males, the COM value in males is also only predicted by anthropometric measurements, meaning that this value is also independent of age and obesity status.

3.4.4 Upper Arm

The upper arm prediction models in females are interesting because the COM prediction does not use any age or BMI terms, while the R_G prediction does not use any anthropometric measures. The female R_G model is the only one in the study which does not improve on the previous prediction method, because none of the new terms are included, while the non-significant age and BMI terms are removed. Although the female COM predictions only included waist and elbow circumferences, the new model more than doubled the amount of variation explained by the previous one using age and BMI terms, meaning that arm COM is another parameters that is only dependent on individual geometry.

Arm COM in males included only age terms and the upper arm circumference, indicating that the COM location is independent of obesity, but varies with age and upper arm size. Both upper arm mass and R_G include waist and elbow circumferences, and at least one BMI term, meaning that they are dependent on bone structure, as well as whole-body mass distribution.

3.4.5 Forearm

All of the forearm models for males and females retained at least one of the age or BMI terms, as well as wrist or forearm circumferences. With ΔR^2 values as high as 0.4 (female forearm mass, Table 19), and each model including multiple circumference measurements, the forearm predictions appear to be highly dependent on individual anthropometric measures, in addition to the significant age and BMI terms.

Overall, nearly all of the observed statistical models benefitted from including individual anthropometric measurements. In addition to observing the effects of age and BMI, data points such as waist and hip circumference provide additional measures of obesity, and whole body mass distribution. By using randomly selected training and testing data sets, this study was able to develop and validate anthropometry based prediction models for the segment parameters of interest. These anthropometric models were able to predict the parameters more precisely than previous modeling methods (deLeva, 1996). In summary, the findings of the present study provide statistical tools that allow the prediction of BSPs using simple individual characteristics such as age, BMI and body measurements.

Limitations of this study involve the study population, which consisted only of healthy American working aged adults with full time jobs. Factors such as activity levels and overall fitness were not considered, and would likely impact body mass distribution. Because the DXA scans were collected with the participants lying supine, some degree of weight shifting may have occurred, which would not be present during standing. Additionally, for this study the specific segment definition used for the torso was chosen for its applicability to inverse dynamics calculations and individual variability (Merrill et al., 2018), and may not be directly comparable to other methods of trunk segment parameter calculations.

4.0 Impact of the Seated Height to Stature Ratio on Torso Segment Parameters

4.1 Introduction

Static modeling programs such as the Three-Dimensional Static Strength Prediction Program (3DSSPP) have proven to be valuable ergonomic tools for assessing strength capabilities and injury risk (Chaffin, 1997), especially when assessing spinal loading and lower back injury risk during lifting tasks (Dreischarf 2016; Feyen 2000; Rajaei et al. 2015; Russell et al. 2007). In order for static models to calculate representative joint contact force and muscle forces, accurate body segment parameter (BSP) inputs are required. The latest version of 3DSSP uses BSP data sets determined based on values for the American industrial populations, as determined by the University of Michigan Center for Ergonomics (University of Michigan Center for Ergonomics, 2017). Thus, the anthropometric data currently available in 3DSSP do not account for variations in age, obesity, or body shape present in the working population (Durkin and Dowling 2003; Matrangola et al. 2008). With over 60% of the US work force being considered overweight ($25.0 \leq \text{BMI} < 30.0 \text{ kg m}^{-2}$) or obese ($\text{BMI} \geq 30.0 \text{ kg m}^{-2}$) (Hertz 2004), and obesity rates increasing with increasing age, there is a need for BSP sets that account for variations in age and obesity. BSPs predicted using traditional methods do not account for these variations and are inaccurate for older adults, with errors being dependent on gender and mass distribution (Chambers et al. 2011). When considering specifically the American working adult

population, these errors reach as high as 20-30%, based on the age and obesity status of the individuals.

The anthropometric models currently used by 3DSSPP (University of Michigan Center for Ergonomics, 2017) use torso segments split into the torso above and below the fifth lumbar vertebra, however the upcoming version will use torso segments that are split into three segments: thoracic torso, lumbar torso, and pelvis, segmented by the T12 and L5 vertebrae. Previous work has attempted to split the torso into multiple segments (deLeva 1996) based on anatomical landmarks, however updated imaging based methods for working adults have treated the torso as a single segment with combined thoracic and lumbar segments. Because static models such as 3DSSPP determine the lower back compression and shear forces, anthropometric inputs need to include parameters derived from split torso segments, as opposed to using a single segment torso. In addition to accounting for gender, age and obesity status, researchers at the University of Michigan Transportation Research Institute (UMTRI) have created statistical models to describe overall body shape in children (Park and Reed 2015) and adults (Reed and Ebert 2013) for use in automobile applications. These surface models have shown that the ratio of subjects seated height to stature (SHS) has significant predictive effects on the statistical body shape models (Park and Reed 2015). Because of the impact of SHS on overall body shape, this measure may also prove to be an important predictor in determining torso segment parameters for use in ergonomic applications.

The objective of this study is two-fold:

- (1) Use established regression methods of determining body segment parameters to determine BSPs of interest (segment mass, center of mass, and radius of gyration) for the thoracic torso, lumbar torso and pelvis (based on the split torso used in 3DSSPP) and full torso.

(2) Explore the use SHS as a possible statistical predictor of these parameters in working adults.

The findings of this study will be used in ergonomic modeling programs including 3DSSPP to predict with a greater accuracy lower back forces, strength capabilities, and injury risks in populations of varying age, obesity status and overall body shape.

4.2 Methods

4.2.1 Study Population

A total of 280 working adults participated in this study (Table 21). Participants were recruited according to gender, age, and BMI, in order to attempt to enroll equal numbers in four BMI categories (normal weight: $18.5 \leq \text{BMI} < 25.0$, overweight: $25.0 \leq \text{BMI} < 30.0$, obese: $30.0 \leq \text{BMI} < 40.0$, and morbidly obese $\text{BMI} \geq 40.0 \text{ kg m}^{-2}$) across three age groups ($21 \leq \text{age} < 40$), middle ($40 \leq \text{age} < 55$), and old ($55 \leq \text{age} < 70$). After obtaining informed written consent, each participant had his or her height and mass recorded to confirm eligibility based on BMI. Female participants of child bearing age were then required to complete a pregnancy test, with a negative result being required for eligibility. A whole body DXA scan (Hologic QDR 1000/W, Bedford, MA, USA) of each participant was then collected using the same methods used in prior studies (Chambers et al. 2010; Chambers et al. 2011; Merrill et al, 2018), with the participant lying supine as shown in Figure 4.

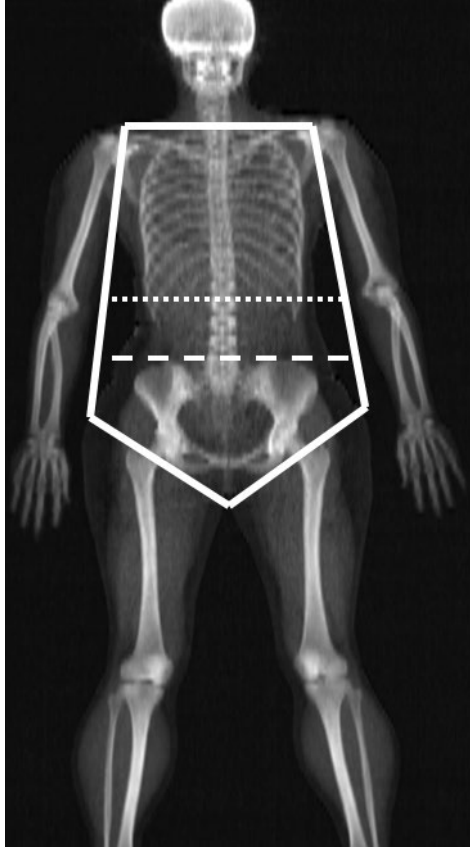


Figure 4: Sample DXA scan with torso delineation. The solid white lines separate the torso segment from the rest of the body. The thoracic torso segment is between the superior torso boundary and the dotted line. The lumbar segment is between the dotted and dashed lines, and the pelvis segment is the inferior section below the inferior dashed line. The full torso segment is between the superior torso boundary and the dashed line.

DXA scan processing procedures consisted of the torso first being separated from the rest of the body using anatomical landmarks and planes (Chambers et al. 2010; Merrill et al. 2018), as shown in Figure 4. Next, based on the anthropometric requirements of the 3DSSP software, the torso was split into the thoracic, lumbar, and pelvis segments, with the thoracic segment ending at the T12/L1 juncture, and the lumbar segment ending at the superior border of the ilium. Each segment was split into 3.9 cm tall slices horizontal slices, in a similar method as described by Ganley and Powers (2004). Pixel densities had assumed values of 2.5-3.0 g cm⁻³ for bone, 0.9 g cm⁻³ for fat, and 1.08 g cm⁻³ for lean tissue. The segment mass, center of mass (COM) and radius of gyration (R_G) were then calculated from the known slice heights and masses using a custom MATLAB script (Mathworks, Natick, MA, USA). Values for segment mass were reported as percent of the total body mass. COM locations were reported as percent of the segment length, where a higher value indicates that the COM is located further in the inferior direction. The R_G values were also reported as percent of the segment length, with the R_G location being measured from the calculated COM. The seated height to stature ratio (SHS) was estimated as follows:

$$SHS = 1 - \frac{Hip\ height\ (cm)}{Stature\ (cm)}$$

Table 21: Descriptive statistics for the study population. Values are given as mean \pm sd.

	All	Female	Male
N	280	148	132
Age (years)	44.9 \pm 13.4	45.8 \pm 13.2	44.0 \pm 13.6
Mass (kg)	89.7 \pm 24.4	85.0 \pm 23.3	94.9 \pm 24.6
Height (cm)	169.6 \pm 9.2	163.5 \pm 6.1	176.5 \pm 6.9
BMI (kg m⁻²)	31.1 \pm 8.1	31.8 \pm 8.7	30.4 \pm 7.2
SHS	0.492 \pm 0.018	0.490 \pm 0.019	0.494 \pm 0.017

4.2.2 Statistical Analysis

The statistical analyses were conducted using JMP Pro 12[®] (SAS Institute, Cary, NC, USA) with statistical significance set at $\alpha = 0.05$. All analyses were stratified by gender due to the significant differences in BSPs between male and female participants. Parameters of interest were checked for normality, and log transformed as necessary prior to further analysis. For each of the parameters, linear regression models were first fit using BMI and age (linear and quadratic terms), as well as their interactions. Next, SHS and its interactions with age and BMI were added to the models.

The coefficient of determination (R^2) and its increases from models only including age and BMI terms to models including SHS-related terms (ΔR^2) were used to describe the added benefit in adding SHS to the predictive models. Nested F-tests were used to describe the significance of including SHS and its interactions with age and BMI beyond the initial models

only using age and BMI terms. The nested F-tests were employed in order to quantify the overall significance of adding the SHS and interaction terms together, as opposed to analyzing the significance of adding the terms separately.

4.3 Results

The study population consisted of 280 working adults (148 female) ages 21-70 (mean: 44.9 ± 13.4 years), as shown in Table 21. The results showed that age, BMI, SHS, and their interactions had several significant associations with the full torso, thoracic torso, lumbar torso, and pelvis segment parameters (Tables 22 and 23).

Age and BMI terms alone explained between 7 and 64 percent of the variability in the parameters in men, and between 5 and 47 percent in women (Table 24). Increased BMI was associated with increased thoracic and full torso mass in women, however it did not have a significant effect on any of the mass parameters in men. When observing the COM and radius of gyration, BMI had a significant effect on several of these parameters in men and women. Age alone did not have any significant relationships with the parameters of interest in women, however it did have a significant association with the thoracic radius of gyration in men, with the values decreasing as age increased.

Adding the SHS terms had significant effects on 2 out of the 12 parameters in men, and 6 out of 12 in women, as determined from the nested F test. The inclusion of the SHS terms explained an additional 0.2-6% of the variability in men, and 0.4-9% of the variability in women (Table 24). The regression models for males had greater variability explained by the age

and BMI terms than for females for 10 out of the 12 parameters, however the models for females demonstrated larger improvements from adding the SHS terms for 8 out of 12 parameters.

Table 22: Regression results for females. Bolded values indicate P < 0.05.

FEMALE	Thoracic M		Thoracic COM		Thoracic Rg	
	P	$\beta \pm SE$	P	$\beta \pm SE$	P	$\beta \pm SE$
Int	0.589	56.991 \pm 6.803	<0.0001	79.243 \pm 5.186	<0.0001	18.714 \pm 1.807
Age	0.097	-2.632 \pm 0.110	0.770	0.174 \pm 0.084	0.453	0.338 \pm 0.029
BMI	0.012	-3.179 \pm 0.179	0.005	-0.395 \pm 0.136	0.0002	0.274 \pm 0.048
Age ²	0.161	3.30E-02 \pm 1.24E-03	0.458	2.06E-03 \pm 9.47E-04	0.347	-5.39E-03 \pm 3.30E-04
BMI ²	0.012	3.65E-02 \pm 2.68E-03	0.020	-1.70E-02 \pm 2.04E-03	0.001	1.69E-03 \pm 7.12E-04
Age*BMI	0.076	0.170 \pm 0.095	0.829	-0.016 \pm 0.072	0.527	-0.016 \pm 0.025
Age*BMI ²	0.114	-2.24E-03 \pm 1.41E-03	0.700	4.14E-04 \pm 1.07E-03	0.693	1.48E-04 \pm 3.73E-04
Age ² *BMI	0.065	-1.98E-03 \pm 1.07E-03	0.942	5.93E-05 \pm 8.12E-04	0.381	2.49E-04 \pm 2.83E-04
Age ² *BMI ²	0.096	2.61E-05 \pm 0.000	0.802	-2.98E-06 \pm 1.19E-05	0.528	-2.61E-06 \pm 4.13E-06
SHS	0.038	16.669 \pm 10.579	0.989	-74.970 \pm 8.064	0.662	14.251 \pm 2.810
SHS*Age	0.664	-0.349 \pm 0.802	0.616	-0.307 \pm 0.611	0.746	0.069 \pm 0.213
SHS*BMI	0.602	0.677 \pm 1.296	0.005	2.795 \pm 0.988	0.091	-0.586 \pm 0.344

	Lumbar M		Lumbar COM		Lumbar Rg	
	P	$\beta \pm SE$	P	$\beta \pm SE$	P	$\beta \pm SE$
Int	0.129	-35.690 \pm 5.782	<0.0001	18.220 \pm 3.059	<0.0001	23.275 \pm 1.202
Age	0.094	1.445 \pm 0.093	0.149	0.447 \pm 0.049	0.740	0.319 \pm 0.019
BMI	0.133	1.352 \pm 0.152	0.045	1.129 \pm 0.080	0.294	0.232 \pm 0.032
Age ²	0.142	-1.39E-02 \pm 1.06E-03	0.164	-1.94E-03 \pm 5.59E-04	0.548	-3.40E-03 \pm 2.19E-04
BMI ²	0.218	-2.40E-02 \pm 2.28E-03	0.193	-1.04E-02 \pm 1.21E-03	0.563	-4.66E-03 \pm 4.74E-04
Age*BMI	0.404	-0.068 \pm 0.081	0.626	-0.021 \pm 0.043	0.319	-0.017 \pm 0.017
Age*BMI ²	0.366	1.08E-03 \pm 1.19E-03	0.628	3.07E-04 \pm 6.32E-04	0.323	2.46E-04 \pm 2.48E-04
Age ² *BMI	0.370	8.14E-04 \pm 9.05E-04	0.733	1.64E-04 \pm 4.79E-04	0.294	1.98E-04 \pm 1.88E-04
Age ² *BMI ²	0.346	-1.25E-05 \pm 1.32E-05	0.743	-2.30E-06 \pm 7.00E-06	0.312	-2.79E-06 \pm 2.75E-06
SHS	0.005	46.533 \pm 8.992	0.801	43.533 \pm 4.757	0.788	1.160 \pm 1.869
SHS*Age	0.354	-0.634 \pm 0.682	0.291	-0.382 \pm 0.361	0.516	-0.092 \pm 0.142
SHS*BMI	0.810	0.265 \pm 1.102	0.183	-0.780 \pm 0.583	0.625	0.112 \pm 0.229

	Pelvis M		Pelvis COM		Pelvis Rg	
	P	$\beta \pm SE$	P	$\beta \pm SE$	P	$\beta \pm SE$
Int	0.086	55.863 \pm 5.191	<0.0001	48.044 \pm 8.159	<0.0001	14.446 \pm 3.867
Age	0.673	1.160 \pm 0.084	0.657	-1.177 \pm 0.132	0.482	-0.199 \pm 0.062
BMI	0.867	-0.917 \pm 0.136	0.0001	-0.434 \pm 0.215	0.485	0.526 \pm 0.102
Age ²	0.935	-1.84E-02 \pm 9.48E-04	0.627	1.09E-03 \pm 1.49E-03	0.492	-4.07E-04 \pm 7.06E-04
BMI ²	0.482	-0.015 \pm 2.05E-03	0.0003	0.038 \pm 3.22E-03	0.297	5.54E-03 \pm 1.52E-03
Age*BMI	0.287	-0.078 \pm 0.073	0.714	0.042 \pm 0.114	0.937	4.28E-03 \pm 0.054
Age*BMI ²	0.264	1.20E-03 \pm 1.07E-03	0.658	-7.48E-04 \pm 1.69E-03	0.871	-1.30E-04 \pm 7.99E-04
Age ² *BMI	0.144	1.19E-03 \pm 8.13E-04	0.889	-1.79E-04 \pm 1.28E-03	0.957	-3.28E-05 \pm 6.05E-04
Age ² *BMI ²	0.130	-1.80E-05 \pm 1.19E-05	0.849	3.55E-06 \pm 1.87E-05	0.920	8.85E-07 \pm 8.84E-06
SHS	0.050	-103.417 \pm 8.072	0.211	-15.948 \pm 12.689	0.206	15.856 \pm 6.014
SHS*Age	0.901	0.076 \pm 0.612	0.130	1.465 \pm 0.962	0.270	0.505 \pm 0.456
SHS*BMI	0.0003	3.641 \pm 0.989	0.013	-3.932 \pm 1.555	0.049	-1.466 \pm 0.737

	Full Torso M		Full Torso COM		Full Torso Rg	
	P	$\beta \pm SE$	P	$\beta \pm SE$	P	$\beta \pm SE$
Int	0.150	21.301 \pm 8.655	<0.0001	30.837 \pm 4.227	<0.0001	8.619 \pm 1.671
Age	0.016	-1.188 \pm 0.140	0.496	1.647 \pm 0.068	0.943	0.301 \pm 0.027
BMI	0.003	-1.827 \pm 0.228	0.023	1.521 \pm 0.111	0.008	0.552 \pm 0.044
Age ²	0.038	0.019 \pm 0.002	0.183	-1.39E-02 \pm 7.72E-04	0.682	-4.03E-03 \pm 3.05E-04
BMI ²	0.005	0.012 \pm 0.003	0.140	-3.48E-02 \pm 1.67E-03	0.016	5.60E-04 \pm 6.58E-04
Age*BMI	0.398	0.103 \pm 0.121	0.111	-0.095 \pm 0.059	0.585	-0.013 \pm 0.023
Age*BMI ²	0.520	-1.15E-03 \pm 1.79E-03	0.104	1.43E-03 \pm 8.73E-04	0.760	1.06E-04 \pm 3.45E-04
Age ² *BMI	0.391	-1.17E-03 \pm 1.36E-03	0.147	9.66E-04 \pm 6.62E-04	0.494	1.80E-04 \pm 2.62E-04
Age ² *BMI ²	0.495	1.36E-05 \pm 1.98E-05	0.134	-1.46E-05 \pm 9.66E-06	0.663	-1.67E-06 \pm 3.82E-06
SHS	0.001	63.202 \pm 13.460	0.447	-31.128 \pm 6.573	0.773	33.483 \pm 2.599
SHS*Age	0.337	-0.982 \pm 1.020	0.351	-0.466 \pm 0.498	0.934	-0.016 \pm 0.197
SHS*BMI	0.569	0.942 \pm 1.649	0.027	1.807 \pm 0.806	0.002	-1.005 \pm 0.318

Table 23: Regression results for males. Bolded values indicate P < 0.05.

MALE	Thoracic M		Thoracic COM		Thoracic Rg	
	P	$\beta \pm SE$	P	$\beta \pm SE$	P	$\beta \pm SE$
Int	0.005	-29.546 ± 6.320	<0.0001	13.114 ± 4.213	<0.0001	35.828 ± 1.280
Age	0.106	-0.585 ± 0.090	0.057	0.830 ± 0.060	0.046	-0.141 ± 0.018
BMI	0.726	-0.058 ± 0.212	0.007	1.090 ± 0.141	0.021	-0.012 ± 0.043
Age ²	0.056	1.24E-02 ± 1.04E-03	0.104	-7.68E-03 ± 6.90E-04	0.026	-7.45E-04 ± 2.10E-04
BMI ²	0.709	2.34E-02 ± 3.26E-03	0.075	-1.01E-02 ± 2.17E-03	0.112	5.68E-04 ± 6.60E-04
Age*BMI	0.462	0.080 ± 0.108	0.716	-0.026 ± 0.072	0.798	-5.62E-03 ± 0.022
Age*BMI ²	0.494	-1.14E-03 ± 1.66E-03	0.753	3.50E-04 ± 1.11E-03	0.741	1.12E-04 ± 3.36E-04
Age ² *BMI	0.487	-8.98E-04 ± 1.29E-03	0.680	3.55E-04 ± 8.58E-04	0.682	1.07E-04 ± 2.61E-04
Age ² *BMI ²	0.502	1.32E-05 ± 1.96E-05	0.740	-4.34E-06 ± 1.30E-05	0.600	-2.09E-06 ± 3.96E-06
SHS	0.836	154.453 ± 10.726	0.151	51.032 ± 7.151	0.825	-11.122 ± 2.173
SHS*Age	0.140	-1.185 ± 0.798	0.334	-0.516 ± 0.532	0.039	0.337 ± 0.162
SHS*BMI	0.031	-3.298 ± 1.514	0.558	-0.593 ± 1.009	0.655	-0.137 ± 0.307

	Lumbar M		Lumbar COM		Lumbar Rg	
	P	$\beta \pm SE$	P	$\beta \pm SE$	P	$\beta \pm SE$
Int	0.257	70.813 ± 6.676	<0.0001	70.083 ± 3.790	<0.0001	38.249 ± 1.457
Age	0.742	-3.327 ± 0.095	0.911	-5.61E-01 ± 0.054	0.871	-6.47E-01 ± 0.021
BMI	0.673	-3.920 ± 0.224	0.004	0.157 ± 0.127	0.440	-0.755 ± 0.049
Age ²	0.643	3.50E-02 ± 1.09E-03	0.928	2.38E-03 ± 6.21E-04	0.921	6.59E-03 ± 2.39E-04
BMI ²	0.833	5.64E-02 ± 3.44E-03	0.037	-5.60E-03 ± 1.95E-03	0.577	1.13E-02 ± 7.51E-04
Age*BMI	0.100	0.190 ± 0.114	0.954	3.74E-03 ± 0.065	0.131	0.038 ± 0.025
Age*BMI ²	0.125	-2.71E-03 ± 1.75E-03	0.984	1.97E-05 ± 9.96E-04	0.171	-5.27E-04 ± 3.83E-04
Age ² *BMI	0.126	-2.10E-03 ± 1.36E-03	0.911	-8.62E-05 ± 7.72E-04	0.192	-3.90E-04 ± 2.97E-04
Age ² *BMI ²	0.149	3.00E-05 ± 2.07E-05	0.980	2.97E-07 ± 1.17E-05	0.233	5.40E-06 ± 4.51E-06
SHS	0.022	-3.110 ± 11.332	0.694	-55.954 ± 6.432	0.169	5.654 ± 2.472
SHS*Age	0.556	0.497 ± 0.843	0.068	0.880 ± 0.478	0.903	0.023 ± 0.184
SHS*BMI	0.876	0.251 ± 1.599	0.594	0.485 ± 0.908	0.762	-0.106 ± 0.349

	Pelvis M		Pelvis COM		Pelvis Rg	
	P	$\beta \pm SE$	P	$\beta \pm SE$	P	$\beta \pm SE$
Int	0.008	13.948 ± 5.926	0.0002	5.613 ± 8.836	0.001	13.913 ± 4.285
Age	0.377	-0.033 ± 0.084	0.493	2.166 ± 0.126	0.631	0.572 ± 0.061
BMI	0.186	-0.162 ± 0.199	0.081	1.222 ± 0.296	0.755	0.139 ± 0.144
Age ²	0.806	7.24E-03 ± 9.71E-04	0.472	-2.09E-02 ± 1.45E-03	0.823	-4.38E-03 ± 7.02E-04
BMI ²	0.134	-9.54E-03 ± 3.06E-03	0.242	-2.79E-02 ± 4.55E-03	0.816	-8.03E-03 ± 2.21E-03
Age*BMI	0.983	2.22E-03 ± 0.102	0.465	-0.111 ± 0.152	0.726	-0.026 ± 0.073
Age*BMI ²	0.827	3.41E-04 ± 1.56E-03	0.514	1.52E-03 ± 2.32E-03	0.743	3.69E-04 ± 1.13E-03
Age ² *BMI	0.847	-2.34E-04 ± 1.21E-03	0.520	1.16E-03 ± 1.80E-03	0.756	2.71E-04 ± 8.73E-04
Age ² *BMI ²	0.983	-3.86E-07 ± 1.83E-05	0.563	-1.59E-05 ± 2.73E-05	0.756	-4.12E-06 ± 1.33E-05
SHS	0.744	11.021 ± 10.059	0.120	-2.222 ± 14.998	0.061	-4.473 ± 7.272
SHS*Age	0.432	-0.589 ± 0.748	0.738	-0.374 ± 1.115	0.660	-0.238 ± 0.541
SHS*BMI	0.674	0.599 ± 1.420	0.513	1.388 ± 2.116	0.359	0.946 ± 1.026

	Full Torso M		Full Torso COM		Full Torso Rg	
	P	$\beta \pm SE$	P	$\beta \pm SE$	P	$\beta \pm SE$
Int	0.124	41.266 ± 6.896	<0.0001	35.696 ± 4.178	<0.0001	41.592 ± 1.521
Age	0.073	-3.912 ± 0.098	0.311	0.129 ± 0.060	0.130	-0.321 ± 0.022
BMI	0.930	-3.978 ± 0.231	0.096	0.567 ± 0.140	0.095	-0.240 ± 0.051
Age ²	0.191	4.74E-02 ± 1.13E-03	0.839	1.09E-03 ± 6.84E-04	0.093	2.64E-03 ± 2.49E-04
BMI ²	0.584	0.080 ± 0.004	0.621	-6.77E-03 ± 0.002	0.210	1.60E-03 ± 7.84E-04
Age*BMI	0.025	0.269 ± 0.118	0.945	-0.005 ± 0.072	0.814	0.006 ± 0.026
Age*BMI ²	0.036	-3.85E-03 ± 1.81E-03	0.883	1.62E-04 ± 1.10E-03	0.909	-4.55E-05 ± 4.00E-04
Age ² *BMI	0.035	-3.00E-03 ± 1.41E-03	0.982	-1.90E-05 ± 8.51E-04	0.762	-9.40E-05 ± 3.10E-04
Age ² *BMI ²	0.045	4.32E-05 ± 2.13E-05	0.959	-6.70E-07 ± 1.30E-05	0.889	6.55E-07 ± 4.70E-06
SHS	0.016	151.344 ± 11.705	0.527	15.767 ± 7.091	0.226	-21.267 ± 2.581
SHS*Age	0.431	-0.688 ± 0.870	0.772	-0.153 ± 0.527	0.127	0.295 ± 0.192
SHS*BMI	0.068	-3.047 ± 1.652	0.882	-0.149 ± 1.001	0.642	0.170 ± 0.364

Table 24: R^2 , ΔR^2 , F, and P values for the full regressions including age, BMI, and SHS terms for females (top) and males (bottom). R^2_I is for the initial model only using age and BMI terms, and R^2_F is for the full model also including the SHS terms. ΔR^2 is the additional variation explained by the model when adding the SHS, (SHS x Age), and (SHS x BMI) terms to the model only including the age and BMI terms. The nested F test represents the statistical significance in adding these three terms to the model at the same time. Bolded values indicate $P < 0.05$.

Females	Thoracic Torso			Lumbar Torso			Pelvis			Full Torso		
	M	COM	Rg	M	COM	Rg	M	COM	Rg	M	COM	Rg
R^2_I	0.091	0.293	0.179	0.143	0.212	0.165	0.198	0.125	0.050	0.151	0.474	0.159
R^2_F	0.121	0.334	0.197	0.194	0.229	0.169	0.291	0.184	0.093	0.227	0.497	0.216
ΔR^2	0.030	0.041	0.019	0.051	0.016	0.004	0.092	0.059	0.043	0.076	0.023	0.058
F	1.572	2.758	1.057	2.886	0.968	0.234	5.888	3.296	2.166	4.453	2.117	3.347
P	0.199	0.045	0.369	0.038	0.410	0.873	0.001	0.023	0.095	0.005	0.101	0.021

Males	Thoracic Torso			Lumbar Torso			Pelvis			Full Torso		
	M	COM	Rg	M	COM	Rg	M	COM	Rg	M	COM	Rg
R^2_I	0.071	0.504	0.360	0.476	0.411	0.136	0.246	0.172	0.106	0.387	0.644	0.190
R^2_F	0.132	0.519	0.383	0.500	0.431	0.151	0.251	0.191	0.137	0.439	0.646	0.219
ΔR^2	0.060	0.015	0.022	0.025	0.020	0.015	0.005	0.019	0.031	0.051	0.002	0.028
F	2.787	1.205	1.457	1.967	1.419	0.692	0.262	0.937	1.438	3.652	0.175	1.444
P	0.044	0.311	0.230	0.123	0.241	0.559	0.853	0.425	0.235	0.015	0.913	0.234

4.4 Discussion

Overall, the results indicate that there are several significant associations of age, BMI, SHS, and their interactions on the full and split torso segment parameters in working men and women. Because this analysis observes the split torso in addition to the full torso segment, the results can provide more insight into the details of the torso anthropometry.

The results indicate that as BMI increases, this excess mass is accumulated within the torso segment (as indicated by increased torso mass as a percentage of total body mass), however it is not evenly distributed within the torso, leading to differing COM and radius of gyration values. Specifically, these changes can be observed in the COM locations for all four segments in women. With increasing BMI, the COM values all move further in the inferior direction with the exception of the pelvis segment, which exhibits a superior shift in COM. When viewed together with the significantly decreasing radius of gyration values (meaning the radius of gyration is closer to the segment center of mass) for the thoracic and full torso, it appears that the additional mass in women accumulates primarily in the same locations in the lower area of the torso. Similar effects can be observed in the thoracic torso segment in men, where increased BMI is correlated with an inferior shift in the COM location, along with a decreased radius of gyration.

The only statistically significant associations of age with the parameters of interest were observed in full torso mass in women, and thoracic torso radius of gyration in men. Similar to the effects of increasing BMI in women, the increase in age corresponds to greater full torso mass as a percent of total body mass, indicating that even when BMI does not change, overall mass distribution may change with age. With increasing age in men, the results are again analogous to increasing BMI, with the radius of gyration values decreasing, meaning that the segment mass tends to accumulate in a specific region, as opposed to throughout the whole segment. Because lean body mass and bone density tends to decrease with age (Atlantis et al., 2008; Jackson et al., 2012, St-Onge, 2005), the results indicate that individuals with similar BMI at different ages will likely have increased adipose tissue, which will contribute towards larger

torso mass percentage and mass distribution, similar to that observed in individuals with increased BMI.

Additionally, the results indicate that the inclusion of the SHS metric, along with its interactions with age and BMI, explains a small but sometimes significant amount of additional variability beyond the variability explained by age and BMI alone. The SHS term had a significant effect on the full torso mass and lumbar torso mass in men and women, however it only had a significant effect on thoracic torso mass in women. Because a larger SHS reflects a longer torso relative to total stature, these effects of higher SHS on full torso mass (as a percentage of body mass) would be expected. By performing this statistical analysis on the split torso parameters, the results show that both genders exhibit increased lumbar torso mass with increased SHS, while men do not demonstrate any relative increases in thoracic torso mass with increased SHS, indicating that individuals with longer torsos relative to total height have differing increases in mass distribution based on sex.

The addition of the SHS and interaction terms to initial models only using age and BMI can provide significant improvement in variability explained in split torso parameters, especially in women. While the increased segment masses would be expected due to the SHS indicating a longer torso relative to height, the collective SHS terms had significant relationships with the thoracic torso and pelvis COM locations, as well as the full torso radius of gyration in women. More precisely, the SHS x BMI interaction was significantly associated with each of these parameters, correlating with an inferior shift in thoracic COM, a superior shift in pelvis COM, and a decrease in full torso radius of gyration. Because these effects are all in the same direction as those seen with increasing BMI, it appears that having an overall body shape characterized by a greater SHS tends to exacerbate the effects on increasing BMI on these parameters.

In order to determine the effect of these age, BMI, and SHS associated parameters on ergonomic calculations, a sensitivity analysis was performed for a lifting task in 3DSSPP (version 6.0.6), to determine the effects of varying torso and pelvis mass and center of mass on the L5/S1 disc compression forces. Using a 163.5 cm tall female (the average of the female study population) model in the stoop lift position (Figure 5), and a downward force of 65 N on each hand, a total of 10 anthropometry inputs sets were applied: deLeva (1996) parameters at BMI of 20 and 45 kg m⁻² (53.5 and 120.3 kg, respectively), and parameters from the results of this study for ages 25 and 65 years, BMI of 20 and 45 kg m⁻², and SHS of 0.452 and 0.528, corresponding to the mean \pm 2 standard deviations.

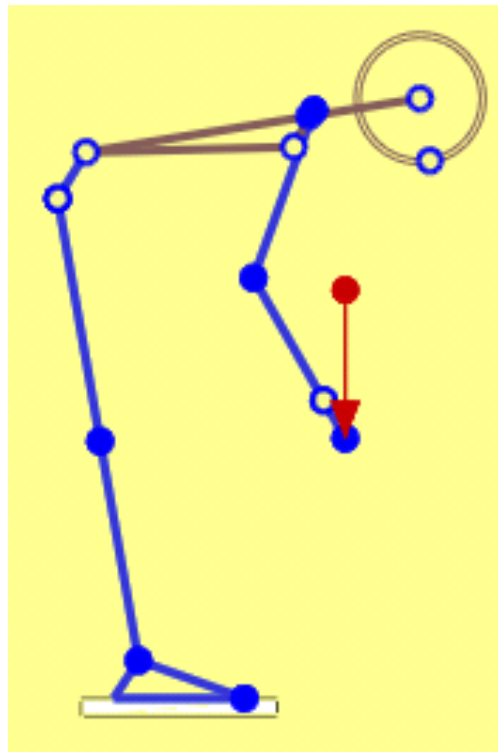


Figure 5: Female model in the stoop lift position.

The results of this sensitivity analysis (Table 25) show that using the deLeva (1996) parameters result in significantly higher predictions for L5/S1 compression force at both BMIs. Within the low BMI group, the compression forces for the 65-year old models were nearly identical at low and high SHS (2132 and 2136 N, respectively), with larger differences appearing between the low and high SHS values for the 25 year old model (2231 vs 2106 N respectively).

Table 25: 3DSSPP sensitivity analysis results. The analysis was performed for females in the stoop lift position, with a 65 N downward force applied to each hand. Compression forces are provided in N.

BMI (kg m⁻²)	L5/S1 Compression					
	20			45		
Group (age in years, or deLeva)	25	65	deLeva	25	65	deLeva
Low SHS	2231	2132	2505	2966	3193	3887
High SHS	2106	2136		3259	3347	

Within the high BMI (45 kg m⁻²) group, the effect of SHS increased at both ages, with high and low compression values of 3347 and 3193 N, respectively for the old group, and 3259 and 2966 N respectively for the young group. Because these results varied by nearly 400 N in the high BMI group, it is important to account for age and body shape, especially for high BMI individuals. These differences in modeling outputs would likely increase for any gait or dynamic lifting, where the differing radius of gyration values would also contribute towards differences in L5/S1 compression calculations.

Limitations for this study include the lack of information regarding fitness history and activity levels within the sample population, meaning that these results may not be representative for athletic or populations with disability. All of the DXA scans were collected with the

participants lying supine, and some amounts of shifting in soft tissue likely occurred from the standing position. Additionally, the statistical regressions resulting from this investigation are not predictive in nature, and should not be used as such; their purpose is to investigate the associations of age, BMI, and SHS with the parameters of interest for potential future inclusion in predictive modeling. Despite these limitations, the findings of this study indicate that age, BMI, and overall body shape as determined from SHS all have significant associations with torso and pelvis segment parameters. Further, the results of the static sensitivity analysis show that these differences need to be included in ergonomic models in order to determine representative lower back compression forces, and their related injury risk.

5.0 Development and Validation of Body Fat Prediction Models in American Adults

5.1 Introduction

Obesity is a growing health concern in the American adult population (Hales et al., 2017), with over 36% of adults over the age of 20 being classified as obese, defined by a body mass index (BMI) of 30.0 kg m^{-2} or greater (Ogden, 2014). Obesity is also a significant factor for health conditions such as knee and hip osteoarthritis and type 2 diabetes, as well as for occupational injuries (Brown and Choi, 2015; Craig et al., 2006; Pollack and Cheskin, 2007), such as falls (Chau et al., 2004) and back injuries (Myers et al., 1999). When considering body fat percentage (BFP) as a measurement of obesity status, high body fat, especially when combined with low BMI, is associated with increased all-cause mortality (Padwal et al., 2016) and cardiovascular disease mortality (Ortega et al., 2016). While approximations of whole-body and abdominal obesity can be approximated with measures such as BMI and waist and hip circumferences, body composition information can provide additional insight into cardiovascular health risks (Ortega et al., 2016).

While measures such as BMI, waist circumference, and waist to hip ratio can approximate body fat percentage and related health risks, imaging methods such as dual energy x-ray absorptiometry (DXA) scanning have been used as direct in-vivo measures of body composition, including body fat percentage (Chambers et al., 2014). Other methods have used

skin fold measurements to model body fat percentage in the general population (Durnin and Womersley, 1974; Jackson and Pollock, 1978; Jackson, Pollock, and Ward, 1980) and the elderly (Chambers et al., 2014; Gause-Nillson and Dey, 2005; Kwok, Woo, and Lau, 2001; Visser, van den Heuvel, and Deurenberg, 1994). These methods have used skin fold to directly predict body fat percentage (Chambers et al., 2014; Gause-Nillson and Dey, 2005; Kwok, Woo, and Lau, 2001), or to predict body density (Durnin and Womersley, 1974; Jackson and Pollock, 1978; Jackson, Pollock, and Ward, 1980; Visser, van den Heuvel, and Deurenberg, 1994), which can then be used to approximate body fat percentage using the two compartment equation developed by Siri (Siri, 1961).

Methods relying only on anthropometric measurements including circumference measurements and height (Hodgdon and Beckett, 1984a; Hodgdon and Beckett, 1984b; Woolcott and Bergman, 2018) have also been employed for the purpose of predicting body fat percentage. These methods have the advantage of accounting for individual body shape, while not requiring the equipment and training necessary to perform skinfold measurements. Specifically, the relative fat mass metric (Woolcott and Bergman, 2018), approximates body fat percentage using only height and waist circumference, making it one of the most simple methods of determining obesity status in American adults. While these established methods have proven effective for military personnel (Hodgdon and Beckett, 1984a; Hodgdon and Beckett, 1984b), and provided improvement over BMI alone in the American adult population (Woolcott and Bergman, 2018), they do not account for the additional effect of age in predicting body composition. When looking at correlations between anthropometric measures such as waist circumference and BMI with body composition, previous research has found that both age and race also play significant roles in predicting body fat percentage (Camhi et al., 2011; Deurenberg, Yap, and van Staveren,

1998; Jackson et al., 2002), and highlights how BMI alone does not provide accurate insight into body composition (Deurenberg, Yap, and van Staveren, 1998).

Due to the wide age and obesity ranges presented in the American adult population (Luckhaupt et al., 2014), the known effects of age and BMI on predicting body composition (Jackson et al., 2002), and the significant predictive abilities of skinfolds (Durnin and Womersley, 1974; Jackson and Pollock, 1978; Jackson, Pollock, and Ward, 1980) and anthropometric measurements (Hodgdon and Beckett, 1984a; Hodgdon and Beckett, 1984b; Woolcott and Bergman, 2018) on body composition, accurate statistical models should attempt to include all of these inputs. The objective of this study was to develop statistical regression models to predict body fat percentage in working men and women using all of these parameters, in order to develop a clinical tool that will provide the most accurate results, and improve over the existing prediction methods without the need for expensive imaging equipment.

5.2 Methods

A total of 228 working adults (116 female) ages 21-70 (mean: 44.4 ± 13.7 years, Table 26) participated in this study. Recruitment was stratified by BMI group, age group and gender to ensure a comprehensive representation of the current working population. More specifically, male and female participants were recruited in equal numbers in three BMI categories (normal weight: $18.5 \leq \text{BMI} < 25.0$, overweight: $25.0 \leq \text{BMI} < 30.0$, and obese: $30.0 \leq \text{BMI} < 40.0$) across three age groups: young ($21 \leq \text{age} < 40$), middle ($40 \leq \text{age} < 55$), and old ($55 \leq \text{age} < 70$).

The study was approved by the University of Pittsburgh Institutional Review Board, and written informed consent was obtained prior to any data collection.

Table 26: Descriptive statistics for the study population. Values are shown as mean (sd).

	N	Age (y)	Mass (kg)	Height (cm)	BMI (kg m⁻²)	Asian (%)	Black (%)	White (%)
All	228	44.4 (13.7)	81.3 (17.3)	170.0 (9.1)	28.0 (4.9)	3	30	67
Female	116	45.6 (13.5)	75.3 (14.4)	163.8 (5.9)	28.0 (5.0)	1	34	65
Male	112	43.2 (13.8)	87.5 (17.8)	176.5 (7.1)	28.0 (4.9)	4	26	70

Each participant had his or her height and mass recorded in order to confirm eligibility based on BMI. Female participants of child bearing age were then required to complete a pregnancy test, with a negative result being required for eligibility. Next, nine skinfold and thirteen anthropometric measurements were collected (Table 27). All of the arm and leg measurements were collected for the right sides only. Each measurement was collected three times, and the average of the three was used for analysis. A whole body DXA scan (Hologic QDR 1000/W, Bedford, MA, USA) of each participant was then collected using the same methods used in prior studies (Chambers et al., 2014), with the participant lying supine as shown in Figure 1. Body fat percentage was determined from the scan as total fat mass divided by total body mass.

Before starting the statistical analysis, the full data set of 228 participants was randomly split into two subgroups: the training set, which contained 163 participants, and the testing set, which contained the remaining 65, with each set containing similar age and BMI distributions

(Table 28). The two groups were used to first develop prediction models (training set), and validate the models (testing set).

All analyses were performed in JMP Pro 12 (SAS Institute, Cary, NC, USA). Specifically, a backwards elimination regression analysis was performed on the whole body DXA determined body fat percentage in the training subset within each gender group. The initial regression model contained age, BMI, age² and BMI² and all their interaction terms, all skinfold measurements, and circumferences of the neck, waist, hips, and limbs. In each step of the analysis, the predictor with the largest P-value was removed, and the analysis was repeated. This process of removing the least significant predictor and repeating the analysis continued until the p-values for all predictors were below 0.10.

Once the training set model was finalized, it was applied to the anthropometric measures in the testing set, so that the predicted and actual segment parameters could be compared in the testing set, and used as a method of validating the models. For comparison purposes, several previously validated body fat estimation methods were also applied to the testing data set. These methods included those determined by Durnin and Womersly (1974), Hodgdon (1984a; 1984b), Jackson and Pollock (1978; 1980), and Woolcott (2018). Within the testing set, the actual and predicted values were compared by calculating the absolute percent error, as well as the root mean square error (RMSE). The actual body fat percentage values were compared to the new and existing prediction models in order to determine the average difference in predicted body fat value, Δ BFP. Within each gender, t-tests were performed between each prediction method and the DXA measured body fat to determine if there were any significant differences, with statistical significance set at $\alpha = 0.05$.

Table 27: Anthropometric measures collected for body fat prediction.

Anthropometric variable	Definition
Chest skinfold	Diagonal fold at 45 degree angle: one half the distance between the anterior axillary line and the nipple for men, one third the distance between the anterior axillary line and the nipple for women
Mid-axillary skinfold	Vertical fold, on the mid-axillary line at the level of the xyphoid process of the sternum
Triceps skinfold	Vertical fold, on the posterior midline of the upper arm, halfway between the acromion and olecranon processes, with the arm held freely to the side of the body
Biceps skinfold	Vertical fold; on the anterior aspect of the arm over the belly of the biceps muscle, 1 cm above the level used to mark the triceps site
Subscapular skinfold	Diagonal fold; 1 to 2 cm below the inferior angle of the scapula
Vertical abdominal skinfold	Vertical fold; 2 cm to the right of the umbilicus
Horizontal abdominal skinfold	Horizontal fold; 2 cm to the right of the umbilicus
Suprailiac skinfold	Diagonal fold; in line with the natural angle of the iliac crest taken in the anterior axillary line immediately superior to the iliac crest
Thigh skinfold	Vertical fold; on the anterior midline of the thigh, midway between the proximal border of the patella and the inguinal crease (hip)
Waist circumference	Circumference at the umbilicus
Hip circumference	Around largest part of the hip
Upper thigh circumference	Around proximal thigh
Mid-thigh circumference	Around point midway between proximal border of patella and inguinal crease
Lower thigh circumference	Around thigh 1 cm above proximal border of patella
Knee circumference	Around medial and lateral femoral epicondyles
Calf circumference	Around largest part of calf
Ankle circumference	Around medial and lateral malleoli
Upper arm circumference	Around midpoint between acromion and olecranon processes
Elbow circumference	Around medial and lateral humeral epicondyles
Lower arm circumference	Around midpoint between lateral humeral epicondyle and ulnar styloid process
Wrist circumference	Around radial and ulnar styloid processes
Hand thickness	Thickness at center of palm

Table 28: Descriptive statistics for the training and testing subsets. Values are shown as mean (sd).

	N	Female	Age (y)	BMI (kg m⁻²)	BFP
All	228	117	44.4 (13.7)	28.0 (4.9)	29.3 (9.2)
Training	163	82	44.3 (13.9)	28.1 (5.1)	29.2 (9.2)
Testing	65	35	44.7 (13.2)	27.7 (4.6)	29.5 (9.1)

5.3 Results

The final models predicted total body fat percentage within the testing subgroup with a root mean square error (RMSE) of 10.6% (Figure 6), compared to the Hodgdon, Durnin, Jackson, and Woolcott prediction methods, which had RMSE of 17.3, 29.7, 15.6, and 19.4%, respectively. When directly comparing the body fat predictions to the DXA measured values, the Durnin and Woolcott predictions significantly overestimated body fat for males and females (Figure 7). The Hodgdon formula significantly overestimated female body fat, and significantly underestimated male body fat, and the Jackson method significantly underestimated only female body fat. Compared to the DXA measured values, the new prediction formula (Equations 5-1 and 5-2) showed a Δ BFP of less than 0.10% for both males and females (Figure 7), and average absolute errors of less than 10% (Table 29). For both equations, all circumference and skinfold measurements are measured in cm.

Equation (5-1)

$$\begin{aligned}\text{Female BFP} = & 225.43 - \text{Age} \cdot 12.42 + (\text{Age}^2) \cdot 0.140 - \text{BMI} \cdot 14.43 + (\text{BMI}^2) \cdot 0.266 + \\ & (\text{Age} \cdot \text{BMI}) \cdot 0.893 - (\text{Age} \cdot \text{BMI}^2) \cdot 0.0154 - (\text{Age}^2 \cdot \text{BMI}) \cdot 0.0100 + (\text{Age}^2 \cdot \text{BMI}^2) \cdot 0.000174 + \\ & (\text{Waist circumference}) \cdot 0.129 - (\text{Hand thickness}) \cdot 6.44 - (\text{Vertical abdominal skinfold}) \cdot 1.83 + \\ & (\text{Thigh skinfold}) \cdot 1.61\end{aligned}$$

Equation (5-2)

$$\begin{aligned}\text{Male BFP} = & 22.76 + \text{Age}^2 \cdot 0.00168 - \text{BMI} \cdot 0.700 + (\text{BMI}^2) \cdot 0.0139 - (\text{Age}^2 \cdot \text{BMI}) \cdot 0.000233 + \\ & (\text{Age}^2 \cdot \text{BMI}^2) \cdot 0.0000072 + (\text{Hip circumference}) \cdot 0.288 - (\text{Mid-thigh circumference}) \cdot 0.401 - \\ & (\text{Hand thickness}) \cdot 4.94 + (\text{Subscapular skinfold}) \cdot 2.22 + (\text{Vertical abdominal skinfold}) \cdot 1.60 + \\ & (\text{Thigh skinfold}) \cdot 1.69\end{aligned}$$

The final prediction models included several age and BMI terms for males and females, and accounted for over 80% of the variation in body fat percentage, with R^2 values of 0.85 and 0.87 for females and males, respectively. The only anthropometric measures included in the female model were waist circumference and hand thickness, while the male model included hip and mid-thigh circumference, and hand thickness. Both models also included the vertical abdominal and thigh skinfolds, while only the male model includes the subscapular skinfold.

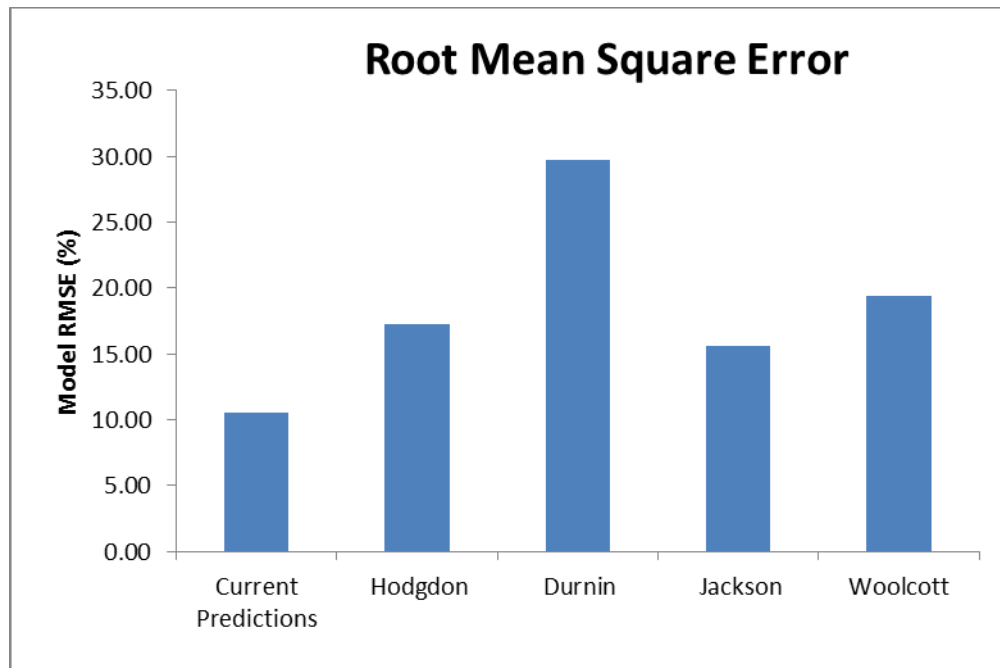


Figure 6: Root mean square error for the testing group for the newly developed prediction model, and the Hodgdon, Durnin, Jackson, and Woolcott models.

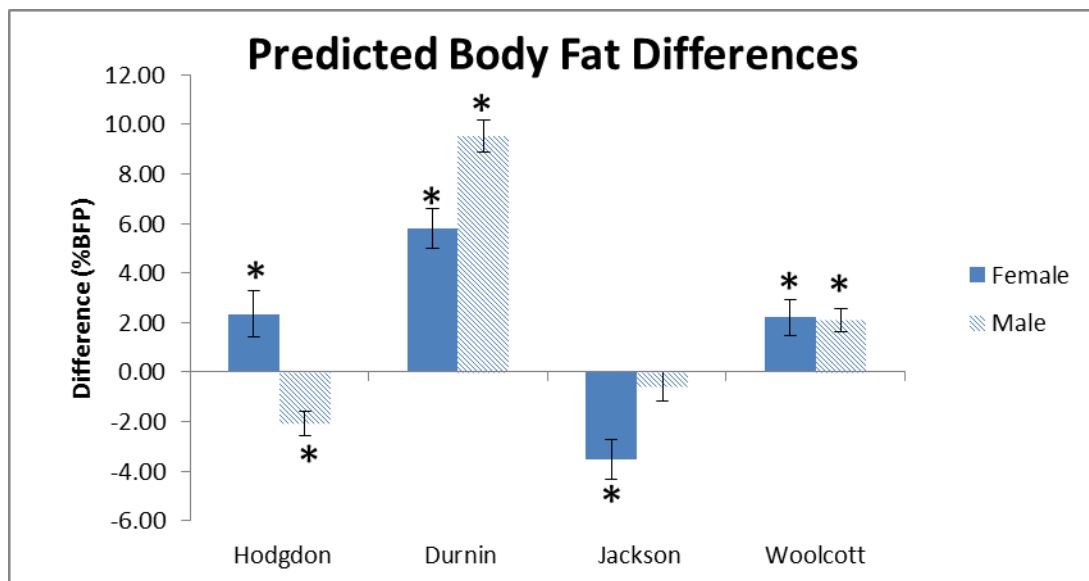


Figure 7: Predicted body fat differences, shown as predicted body fat minus DXA measured body fat for each established prediction method. Error bars represent standard error. * indicates $p < 0.05$ compared to DXA measured values.

Table 29: Average absolute percent errors for each prediction method. Values given as mean (sd). Errors calculated as the absolute difference between prediction methods and DXA measured values, divided by DXA measured values.

	Predicted	Hodgdon	Durnin	Jackson	Woolcott
All	8.7 (7.6)	14.9 (11.3)	33.3 (26.0)	11.3 (8.7)	14.7 (13.8)
Female	8.4 (6.4)	13.2 (9.9)	20.3 (17.1)	12.4 (9.4)	11.2 (11.6)
Male	9.1 (8.9)	16.9 (12.7)	48.5 (26.6)	10.1 (7.8)	18.8 (15.2)

5.4 Discussion

The objective of this study was to develop a new prediction model for body fat estimation in working men and women, accounting for a wide range of ages and obesity levels and variation in individual anthropometry. Compared to previous methods of estimating body fat in adults, this new formula showed greatly improved accuracy in predicting the DXA derived body fat percentage, as demonstrated by the RMSE, Δ BFP, and average absolute errors. The new prediction model is unique among other methods because it includes age, BMI, anthropometric measures, and skinfold measures, while the preexisting methods only use skinfolds (Durnin), anthropometric measurements (Hodgdon and Woolcott), or skinfolds and age (Jackson). Because the backward elimination regression process initially included all of the predictors this study did not suffer from the limitation of being restricted only to specific categories of inputs.

Compared to the established methods of predicting body fat percentage, the new model requires more measurements than the anthropometry-only methods used by Hodgdon (1984a; 1984b) and Woolcott (2018), but with the benefit of providing significantly more accurate predictions in both men and women. While the Woolcott model provides significant improvement (Woolcott and Bergman, 2018) over BMI alone for predicting body composition, it results in estimations that are about two percentage points higher than the new models (Figure 7). The Woolcott (2018) study and this study both used DXA scans to determine the actual body composition in participants, however the Woolcott study observed a larger sample size of American adults, while this study was limited to working adults with full time jobs. Although physical activity information was not collected as part of this study, previous research has indicated that men and women with active full-time jobs, and men with sedentary full time jobs tend to be more active than unemployed adults (Van Domelen et al., 2011), so these potential differences in lifestyles and activity levels between the two study populations may have contributed towards different modeling outcomes for predicting body fat percentage.

A similar comparison issue arises when observing the differences between the Hodgdon (1984a; 1984b) models and the results of this study, due to the Hodgdon models being developed for active duty US Navy personnel. The Hodgdon studies observed participants that were both younger and less obese (Hodgdon 1984a; Hodgdon 1984b) than the participants in this study. Interestingly, this difference in population and models used lead to the Hodgdon method underestimating body fat in males, while overestimating body fat in females, indicating that with the increasing age and BMI, circumference measurements may play different roles in predicting body composition, and skinfold measurements are necessary for providing further predictive ability.

When comparing the Durnin (1974) and Jackson (1978; 1980) skinfold measurement models to the results of this study, the Durnin models greatly overestimated body fat in men and women, while the Jackson model underestimated body fat in women. The Jackson model for men was the only prediction in this comparison to not significantly over or under estimate the DXA scan derived body fat percentage. While both of these studies observed wide age ranges of adults (16-72 years for Durnin, and 18-61 years for Jackson) similar to this study, the study populations both had lower average BMI and body fat percentage, again demonstrating that the results of this study are necessary for use in the American working adult population.

Another major difference between the results of this study and previous skinfold models is that both the Durnin (1974) and Jackson (1978; 1980) models used sums of skinfolds to predict body composition instead of looking at the individual contributions of these variables, while this study observed the contributions of each skinfold site individually. Observing each site individually allows changes in each site to be weighted differently relative to each other. For example, Equation (5-2) (for males) shows that changes in the subscapular skinfold site lead to larger changes in body fat prediction than changes in the abdominal or thigh sites, while the Durnin or Jackson models would treat similar changes in any of the included sites as having the same impact on body fat prediction. The models resulting from this study can therefore account for more of the individual variability in body composition relating to how and where excess body fat is stored, and how this body fat distribution changes with age, gender, and BMI.

The new prediction methods also likely show improved accuracy and clinical relevance over existing methods because of the inclusion of waist (for females) and hip (for males) circumferences in the final models. These measures have been previously established as predicting obesity status, and risk of developing obesity related health issues, such as type 2

diabetes, hypertension, insulin resistance, and dyslipidemia (Despres and Lemieux, 2006; Despres et al., 2008; Folsom et al., 2000; Lee et al., 2008), meaning that in addition to predicting body composition, these models may provide further insight into the development of more serious health risks.

Unlike the other referenced methods of determining body fat, the new regression model employs hand thickness as a predictor for body fat in men and women, with increased hand thickness correlating with decreased body fat percentage. Previous research into hand muscle thickness, grip strength, and body composition has found that increased hand muscle thickness is correlated with increased skeletal muscle mass (Morimoto et al., 2017), while the relationship between grip strength and body composition has yielded mixed or inconclusive results (Ingrova, Kralik, and Bartova, 2017; Lad et al., 2013, Miyatake et al., 2012). The inclusion of hand thickness in the final statistical model is likely significant because it can serve as a proxy for grip strength and whole body muscle mass, and explain body fat percentage when included alongside age and BMI.

While the models developed in this study account for overall body shape (from the waist, hip, and thigh circumferences) and localized body fat distribution (from the subscapular, abdominal, and thigh skinfolds measurements), they also account for the additional changes in body composition associated with age and BMI. The inclusion of age is especially important for accurate composition calculations due to the decrease in lean body mass and bone density that occurs with increasing age (Atlantis et al., 2008; Jackson et al., 2012; St-Onge, 2005). Because the models include this variety of inputs, a trained clinician is likely required to collect the necessary measurements, whereas more simple methods like relative fat mass (Woolcott and Bergman, 2018) can be determined by an individual without any clinical training. The extra

requirements necessary for using these new models mean that they will likely be most useful in a clinical or medical setting where the ultimate goal is to most accurately determine body fat percentage.

There were a few limitations for this study, mostly dependent on the population studied. While the study sample included a wide representation of age, race, and obesity levels, factors such as physical fitness and overall activity levels were not accounted for during recruitment. Because only working adults with full time jobs were eligible to participate in this study, the final prediction models are likely not applicable to special populations such as the elderly or athletes. The population studied was also limited to participants with a BMI of less than 40.0 kg m⁻² due to inaccuracy of abdominal and thigh skinfold measures in morbidly obese individuals, so the results may not be applicable to working adults with extreme levels of obesity. Previous work relying on sums of skinfolds had the advantage of minimizing the inherent errors in skinfold measurements, which may vary by site, while these results offer the advantage of accounting for individual fat distribution at the cost of potentially decreased accuracy in the applications of the models due to the increased dependence on skinfold accuracy.

6.0 Discussion and Conclusions

6.1 Summary

The results of this dissertation highlight the associations of age, obesity, and overall body shape on anthropometry, and present validated predictive models for body segment parameters (BSPs) and body fat. After investigating the initial relationships between age, body mass index (BMI) and the segment parameters of interest (Specific Aim 1), the predictive models were developed in order to produce representative parameter sets in individuals (Specific Aim 2), which are essential for accurate static and dynamic model calculations. Further, the impact of overall body shape as determined by the seated height to stature ratio (SHS) was investigated (Specific Aim 3), which is especially important for ergonomic modeling involving lower back compression and shear forces, and their related risk of injury. Finally, statistical methods similar to those used to predict segment parameters were used to develop predictive models for body fat percentage (Specific Aim 4).

The criteria for Specific Aim 1 were met by first finding that out of 15 total segment parameters, BMI had significant associations with 7 parameters in females, and 6 parameters in males, with R^2 values as high as 0.50. Next, adding the age terms to the models had significant improvements in 8 parameters in females, and 12 in males, explaining an additional 5-20% of the variability. Finally, including the age x BMI interaction terms had smaller impacts on the

analysis, with significant effects on 3 of the parameters in females, and 4 parameters in males, explaining an extra 1-11% of the variability. Overall, the results of this analysis demonstrated that age and BMI both have significant associations with BSPs. While these results are not predictive and should not be used as such, they indicate that age and BMI should be taken into account when developing predictive models.

Specific Aim 2 built on the results of Specific Aim 1 by including the age and BMI terms, along with individual anthropometric measurements, in a backwards elimination regression to develop predictive BSP models. The predictive models resulted in root mean square errors (RMSE) of less than 5% of the mean for all center of mass and radius of gyration parameters, and less than 10% of the mean for forearm, shank, and torso masses. These models showed prediction errors of less than 7.5% for all parameters in males and females, compared to the errors from the established de Leva (1996) data set, which ranged from 6-63%.

Specific Aim 3 contained similar goals to Specific Aim 1, however it also included the SHS ratio, along with age and BMI, and examined split torso parameters. The SHS ratio has been found to be a predictive metric in body surface modeling in work done by the University of Michigan Transportation Research Institute (Park and Reed, 2015; Reed and Ebert, 2013), and serves as a general measurement of overall body shape. While the SHS measurement was not directly collected during the study visits, its approximation based on hip height was compared to the actual SHS value on a sample of lab employees, and the estimation was found to be within 5% of the actual measurement. By adding SHS and its interactions of age and BMI to the models from Specific Aim 1, 6 of the 12 parameters in females, and 2 of the 12 in males showed significant improvements, with the variability explained increasing by up to 9%. Similarly to Specific Aim 1, these results are not predictive models and should not be used as such, however

the results serve as motivation to include SHS when developing predictive BSP models, and determining specific torso parameters in individuals.

Finally, Specific Aim 4 began with a backwards elimination regression process similar to Specific Aim 2, with the goal of developing predictive models to determine body fat percentage. The goal of this aim was to predict body fat percentage as accurately as possible, using a combination of age and BMI terms, along with skinfold and anthropometric measurements. The final models included a combination of several age, BMI, skinfold, and anthropometric measures, and predicted body fat percentage with a RMSE of 10.6% of the mean. Compared to four previously established body fat prediction methods, these models resulted in average errors of less than 10% of the mean, while the other prediction methods (Durnin and Womersly, 1974; Hodgdon and Beckett, 1984a; Hodgdon and Beckett, 1984b; Jackson and Pollock, 1978; Jackson, Pollock, and Ward, 1980; Woolcott and Bergman, 2018) ranged from 10-48%.

Compared to other methods of anthropometric data collection, DXA scanning was selected due to its ability to noninvasively collect in vivo data, at a minimal cost compared to other imaging methods. DXA scanning has proved especially valuable for these studies because it has enabled the calculations of parameters with different boundaries and endpoints (Merrill et al., 2018), as well as the splitting of major torso segments for specific ergonomic applications. Unlike geometric or photogrammetric methods which rely on tissue composition and density assumptions, DXA scan results can directly measure the masses and compositions necessary to determine body fat percentage and anthropometric parameters.

While previous work has shown population level differences based on race in body composition (Camhi et al., 2011) and anthropometry (Shan and Bohn, 2003), it is likely that these differences are due to assumptions regarding tissue density and composition when relying

on geometric methods (Durkin, Dowling, and Scholtes, 2005). Because the population of this study (Table 26) was a reflection of the diversity of the American adult population, all participants were analyzed together, and not separated by race. Because the DXA scanning method allowed the analyses to bypass assumptions of tissue mass and distribution, and included several age, obesity, and geometric predictors, the resulting predictions in Specific Aims 2 and 4 were able to address the adult population as a whole, regardless of race.

6.2 Applications

The most directly applicable sections of this work involve the predictive regressions derived for BSPs and body composition. The static sensitivity analysis, observing the impacts of age, BMI, and SHS (Table 25), demonstrated the effects of varying torso parameters on L5/S1 compression model outputs, and confirmed the need to account for the individual parameters. Further, individual body shape and anthropometric measurements should be used to predict segment parameters for all major body segments in order to calculate representative joint reaction forces and moments.

6.2.1 Sensitivity Analyses

The static sensitivity analysis performed for a lifting task with varying age, BMI, and SHS levels demonstrated the effects of changing anthropometric inputs on calculated L5/S1

compression forces (Table 25), and showed how these calculations differ from those determined from a previously established anthropometric data set. The differences in these outputs appear to be largely driven by the pelvis and torso masses, with increasing masses leading to larger compression calculations. Center of mass locations alone do not appear to be correlated with changes in compression forces, due to the mass and center of mass values being altered together, and not separately in this analysis. Because altering torso center of mass locations leads to smaller differences than comparable changes in torso mass (as a fraction of whole body mass), the differences in torso mass present in the sample data sets being compared contribute more towards the differences in compression calculations.

In order to quantify the effects of segment parameters on dynamic modeling outputs, the predicted thigh and shank segment parameters from Specific Aim 2 for a sample of male participants were applied to a gait trial with an unexpected slip perturbation. The primary outputs for these models were the hip and knee joint reaction forces and moments on the perturbed (left) limb during the slip and response. The eight male participants selected for this analysis covered wide age (26 – 69 years) and BMI (19.90 – 44.34 kg m⁻²) ranges.

For each individual, the predicted thigh and shank parameters were calculated from the final regression models (Tables 15 and 16), and applied to a whole body 3D inverse dynamics model (Moyer, 2006). The variables of interest for this analysis were the peak knee and hip response moments and forces (normalized to body mass), and the resulting differences in the values across subjects. Sample hip moment results are provided in Figure 8. The model outputs have minimal differences (across sets of anthropometric inputs) throughout most of the trial, however the peak flexion moments range from 0.98 to 1.23 Nm kg⁻¹ during the slip response.

The resulting calculated differences (across sets of anthropometric inputs) in hip joint contact forces and moments varied by over 15% of the average for anterior, lateral, and superior forces, and flexion moments (Figures 9 and 10). Differences in knee force and moment outputs were much smaller than the hip, with only the anterior and superior forces showing maximum differences of over 10% of the mean.

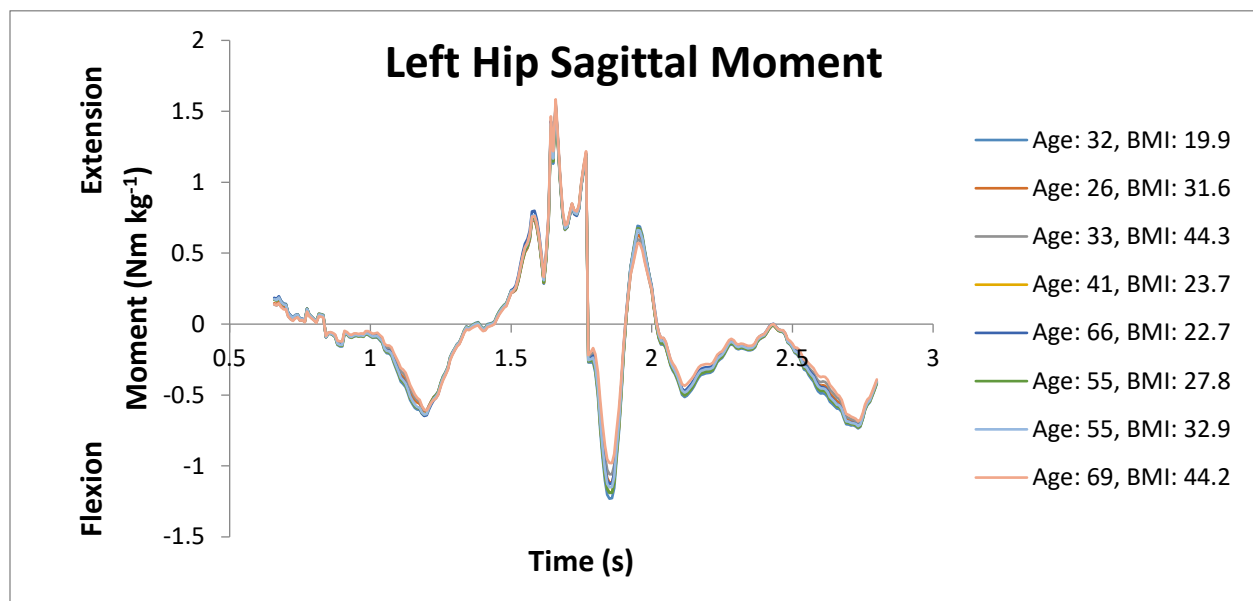


Figure 8: Left hip normalized extension moment outputs during unexpected slip and response for each individual input set. Positive moments represent extension, and negative moments represent flexion.

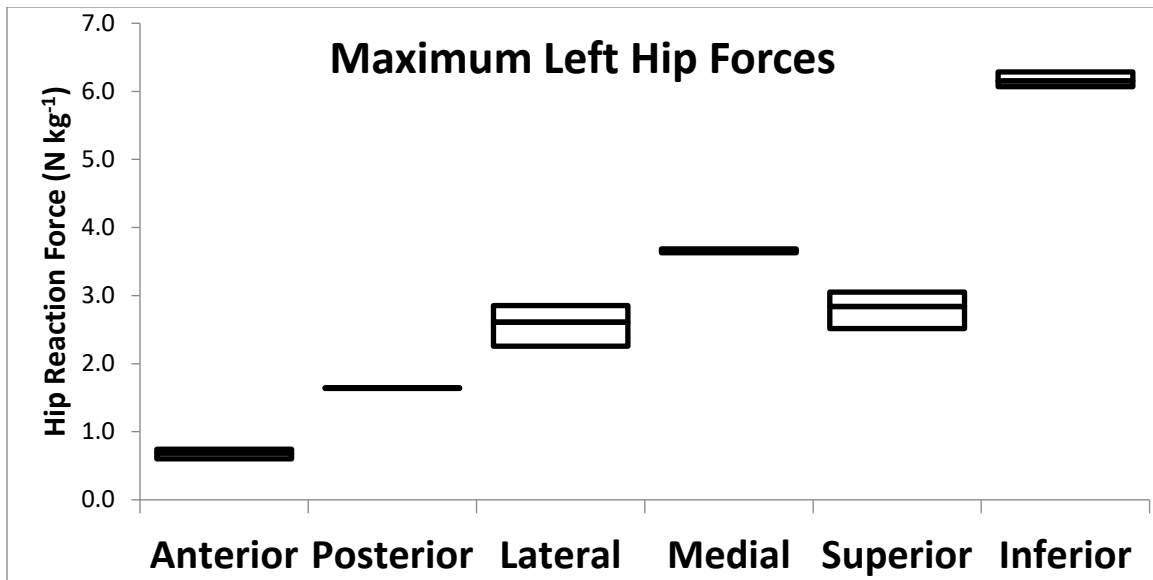


Figure 9: Normalized peak hip reaction forces. Lines shown represent the minimum, average, and maximum model outputs for each measure, across all sets of anthropometric inputs.

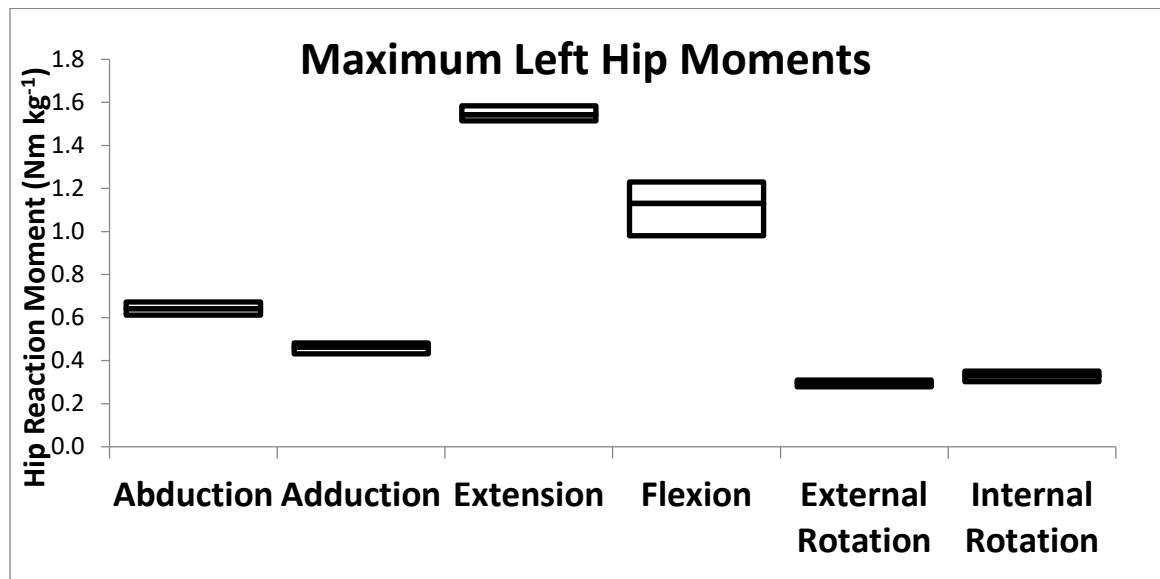


Figure 10: Normalized peak hip reaction moments. Lines shown represent the minimum, average, and maximum model outputs for each measure, across all sets of anthropometric inputs.

While this sensitivity analysis is somewhat limited in that it only observed the changes in knee and hip kinetics, the results for the hip show that the modeling outputs can vary by up to 15-20%, emphasizing the need for representative, individual anthropometric inputs. The magnitudes of the differences observed would likely increase for movements involving larger segments such as the trunk. Because the inverse dynamic model relies on force plate inputs along with kinematic motion capture data, the normalized anthropometric inputs altered were only based on the mass distribution within the body, and within segments, so that the whole body stature and mass did not change between subjects. The results of this dynamic analysis along with the static lifting task serve to underscore the importance of accounting for individual body shape in addition to age and obesity status when predicting anthropometric data for biomechanics applications.

6.2.2 Body Fat Definition of Obesity

Compared to previously established body fat prediction methods (Durnin and Womersly, 1974; Hodgdon and Beckett, 1984a; Hodgdon and Beckett, 1984b; Jackson and Pollock, 1978; Jackson, Pollock, and Ward, 1980; Woolcott and Bergman, 2018), the models developed in Specific Aim 4 proved to be more accurate, as indicated by their smaller RMSE and average errors. While measures such as BMI and waist-hip ratio (WHR) can provide approximations of whole body and abdominal obesity, body composition can provide additional insight into cardiovascular health risks (Ortega et al., 2016). A recently developed method of predicting obesity, relative fat mass (RFM), has proven to be more accurate in obesity predictions than BMI, while being similarly simple to calculate (Woolcott and Bergman, 2018). In order to

observe the relative predictive ability of the body fat models, the DXA scan derived body fat percentages were compared to the obesity classifications of BMI, WHR, RFM, and the predictive models. For defining obesity based on body fat percentage and RFM, the cutoff values determined by Woolcott and Bergman (2018) of 22.8% for males, and 33.9% for females were used, as were WHR cutoff values of 0.85 for females, and 0.90 for males (World Health Organization, 2008). Table 30 shows the number of participants in the testing sub group (n = 65) defined as obese or non-obese by DXA scan derived body fat percentage, compared to the BMI, RFM, WHR, and Specific Aim 4 predicted methods.

Table 30: DXA derived obesity status compared to BMI, RFM, WHR, and Aim 4 predicted models. DXA obesity is determined from the actual values measured, while RFM and Aim 4 obesity is determined from the predictive models. DXA, RFM, and Aim 4 used body fat percentage cutoffs of 22.8% for men, and 33.9% for women. WHR uses obesity cutoffs of 0.85 for women, and 0.90 for men, while BMI uses a cutoff of 30.0 for men and women.

	DXA obese	DXA non obese
BMI obese	19	1
BMI non obese	16	29
RFM obese	34	13
RFM non obese	1	17
WHR obese	23	7
WHR non obese	12	23
Aim 4 predicted obese	32	5
Aim 4 predicted non obese	3	25

Compared to the BMI, RFM, and WHR definitions of obesity, the Aim 4 predicted models proved to be the most accurate, with 88% of the participants classified correctly. The next most accurate method was RFM, with 78% classified correctly. While the RFM method showed a small improvement in accurately diagnosing DXA derived obesity, it incorrectly classified more participants as being obese than the Aim 4 predictions. Compared to the DXA derived body fat percentages, the Aim 4 predictions explained the most variability of the four methods compared, with R^2 values of 0.717 for females, and 0.850 for males.

6.3 Conclusions

The results of this dissertation demonstrate the need to account for age, BMI, and individual characteristics when determining body segment parameters. While the results provided in Specific Aims 1 and 3 are not predictive in nature, and not intended to be used as such, future related work may include developing validated predictive regressions using only age and BMI, so that more general population level parameters may be predicted when specific individual models are not available or necessary. DXA scanning has proven to be an accurate, inexpensive method of determining in vivo composition and segment parameters, and the resulting predictive models translate this information so that it can be used in the absence of access to DXA scanning and analysis systems. Additionally, these scans can be further utilized to describe mass distribution and tissue type by analysis on a pixel by pixel basis, and incorporated with established surface modeling methods to create a more descriptive definition of the body as a whole.

Along with a more detailed scan analysis process, an increase in the sample size would allow for the inclusion of more in depth body measurements utilized for the Specific Aim 2 analysis. For example, torso measurements could include torso circumferences collected the same points as the width and depth measurements, while limb measurements could include circumferences at several points along each segment, as opposed to the current method using only mid-length circumferences. Other measurements such as hip depth (measured in the anterior-posterior direction), when combined with bony landmark measurements such as inter-ASIS distance would provide insight into how soft tissue distribution relative to skeletal structure contributes towards segment parameters and body composition. Because an increase in sample size would allow for an increase in the degrees of freedom available for building predictive statistical models, the additional measurements and their potential interaction with existing measurements could further explain the individual variability in body shape and mass distribution. Improvements in the predictive modeling may be addressed with backwards elimination approaches similar to those used in Specific Aims 2 and 4, or with more advanced machine learning algorithms that have the ability to perform more in depth examinations of potential interactions between anthropometric measurements.

Future work may also address the issue presented by the current DXA collection method, which only uses frontal plane imaging, with participants lying supine. Ideally, scan data should be collected with participants standing upright, as they would be while performing gait and gait perturbation tasks, so that soft tissue distribution is not distorted. Further, three dimensional data collection would allow for the calculation of centers of mass and moments of inertia along all three anatomical axes for each segment. Finally, detailed three dimensional mass and

composition data can be combined with existing surface modeling techniques to create more descriptive full body statistical models.

Bibliography

- Atlantis E., Martin S.A., Haren M.T., Taylor A.W., and Wittert G.A. 2008. "Lifestyle factors associated with age-related differences in body composition: The Florey Adelaide male aging study." *American Journal of Clinical Nutrition* 88: 95-104.
- Bray G.A., DeLany J.P., Volaufova J., Harsha D.W., and Champagne C. 2002. "Prediction of body fat in 12-y-old African American and white children: Evaluation of methods." *American Journal of Clinical Nutrition* 76: 980-990.
- Brown E. and Choi S.D. 2015. "Obesity and the risk for occupational injuries: A literature review." *Journal of Environmental and Occupational Science* 4(3): 163-170.
- Camhi S.M., Bray G.A., Bouchard C., Greenway F.L., Johnson W.D., Newton R.L., Ravussin E., Ryan D.H., Smith S.R. and Katzmarzyk P.T. 2011. "The relationship of waist circumference and BMI to visceral, subcutaneous, and total body fat: Sex and race differences." *Obesity* 19: 402-408.
- Chaffin D.B. 1997. "Development of computerized human static strength simulation model for job design." *Human Factors and Ergonomics in Manufacturing* 7(4): 305-322.
- Chaffin D.B., Andersson G.B.J., and Martin B.J. 2006. *Occupational Biomechanics*. 4th ed. Hoboken, New Jersey: Wiley-Interscience.
- Chaffin D.B. and Muzaffer E. 1991. "Three-dimensional biomechanical Static Strength Prediction Model sensitivity to postural and anthropometric inaccuracies." *IEEE Transactions* 23: 215-227.
- Chambers A.J., Sukits A.L., McCrory J.L., and Cham R. 2010. "The effect of obesity and gender on body segment parameters in older adults." *Clinical Biomechanics* 25: 131-136.
- Chambers A.J., Sukits A.L., McCrory J.L., and Cham R. 2011. "Differences in geriatric anthropometric data between DXA-based subject specific estimates and non-age specific traditional regression models." *Journal of Applied Biomechanics* 27(3):197-206.
- Chambers A.J., Parise E., McCrory J.L., and Cham R. 2014. "A comparison of prediction equations for the estimation of body fat percentage in non-obese and obese older Caucasian adults in the United States." *The Journal of Nutrition, Health, and Aging* 18(6): 586-590.

- Chandler R.F., Clauser C.E., McConville J.T., Reynolds H.M., and Young J.W. 1975. "Investigation of inertial properties of the human body." U.S. Department of Transportation, Washington, DC DOT HS-801 430 /AMRL-TR-74-137.
- Chau N., Gauchard G.C., Siegfried C., Banamghar L., Dangelzer J.L., Fraincais M., Jacquin R., Sourdot A., Perrin P.P., and Mur J.M. 2004. "Relationships of job, age, and life conditions with the causes and severity of occupational injuries in construction workers." *International Archives of Occupation and Environmental Health* 77: 60-66.
- Chen S-C., Hsieh H-J., Lu T-W., and Tseng C-H. 2011. "A method for estimating subject-specific body segment inertial parameters in human movement analysis." *Gait and Posture* 33: 695-700.
- Chiang J., Stephens A., and Potvin J. 2006. "Retooling Jack's Static Strength Prediction Tool," SAE Technical Paper 2006-01-2350.
- Clauser C.E., McConville J.T., and Young J.W. 1969. "Weight, volume, and center of mass of segments of the human body." Technical Report AMRL 69-70, Wright-Patterson Air Force Base, Dayton, Ohio.
- Craig B.N., Congleton J.J., Kerk C.J., Amendola A.A., and Gaines W.G. 2006. "Personal and non-occupational risk factors and occupational injury/illness. *American Journal of Industrial Medicine* 49: 249-260.
- Damavandi M., Farahpour N., and Allard P. 2009. "Determination of body segment masses and centers of mass using a force plate method in individuals of different morphology." *Medical Engineering and Physics* 31: 1187-1194.
- de Leva P. 1996. "Adjustments to Zatsiorsky-Seluyanov's segment inertia parameters." *Journal of Biomechanics* 29: 1223-1230.
- de Looze F.J., Kingma I., Bussmann J.B., and Toussaint H.M. 1992. "Validation of a dynamic linked segment model to calculate joint moments in lifting." *Clinical Biomechanics* 7: 161-169.
- de Looze M.P., Bussmann J.B., Kingma I., and Toussaint H.M. 1992. "Different methods to estimate total power and its components during lifting." *Journal of Biomechanics* 25: 1089-1095.
- Dempster W.T. 1955. "Space requirements of the seated operator," Wright Air Development Center, Wright Patterson Air Force Base, Ohio WADC-TR-55-159.
- Desjardins P., Plamondon A., and Gagnon M. 1998. "Sensitivity analysis of segment models to estimate the net reaction moments at the L5/S1 joint in lifting." *Medical Engineering & Physics* 20: 153-158.
- Despres J.P. and Lemieux I. 2006. "Abdominal obesity and metabolic syndrome." *Nature* 444: 881-887.

- Despres J.P., Lemieux I., Bergeron J., Pibarot P., Mathieu P., Larose E., Rodes-Cabau J., Bertrand O.F., and Poirier P. 2008. "Abdominal obesity and the metabolic syndrome: Contribution to global cardiometabolic risk." *Arteriosclerosis, Thrombosis, and Vascular Biology* 28: 1039-1049.
- Deurenberg R., Yap M., van Staveren W.A. 1998. "Body mass index and percent body fat: A meta-analysis among different ethnic groups." *International Journal of Obesity* 22: 1164-1171.
- Dreischarf M., Shirazi-Adl A., Arjmand N., Rohlmann A., and Schmidt H. 2016. "Estimation of loads on human lumbar spine: A review of in vivo and computational model studies." *Journal of Biomechanics* 49: 833-845.
- Dumas R., Cheze L, and Verriest J-P. 2007. "Adjustments to McConville et al. and Young et al. body segment inertial parameters." *Journal of Biomechanics* 40: 543-553.
- Durkin J.L., and Dowling J.J. 2003. "Analysis of body segment parameter differences between four human populations and the estimation errors of four popular mathematical models." *Journal of Biomechanical Engineering* 125: 515-522.
- Durkin J.L., Dowling J.J., and Scholtes L. 2005. "Using mass distribution information to model the human thigh for body segment parameter estimation." *Journal of Biomechanical Engineering* 127: 455-464.
- Durnin J.V. and Womersley J. 1974. "Body fat assessed from total body density and its estimation from skinfold thickness: Measurements on 481 men and women aged from 16 to 72 years." *British Journal of Nutrition* 32:77-97.
- Feyen R., Liu Y., Chaffin D., Jimmerson., and Joseph B. 2000. "Computer-aided ergonomics: a case study of incorporating ergonomic analyses into workplace design." *Applied Ergonomics* 31: 291-300.
- Folsom A.R., Kushi L.H., Anderson K.E., Mink P.J., Olson J.E., Hong C.P., Sellers T.A., Lazovich D., and Prineas R.J. 2000. "Associations of general and abdominal obesity with multiple health outcomes in older women." *Archives of Internal Medicine* 160: 2117-2128.
- Ganley K.J. and Powers C.M. 2004. "Anthropometric parameters in children: a comparison of values obtained from dual energy x-ray absorptiometry and cadaver-based estimates." *Gait and Posture* 19: 133-140.
- Gauchard G.C., Chau N., Touron C., Benamghar L., Dehaene D., Perrin P.P., and Mur J.M. 2003. "Individual characteristics in occupational accidents due to imbalance: A case-control study of the employees of a railway company." *Occupational and Environmental Medicine* 60: 330-335.
- Gause-Nilsson I. and Dey D.K. 2005. "Percent body fat estimation from skin fold thickness in the elderly. Development of a population-based prediction equation and comparison with

- published equations in 75-year-olds.” *The Journal of Nutrition, Health and Aging* 9:19-24.
- Gu J.K., Charles L.E., Andrew M.E., Ma C.C., Hartley T.A., Violanti J.M., and Burchfiel C.M. 2016. “Prevalence of work-site injuries and relationship between obesity and injury among US workers.” *Journal of Safety Research* 58: 21-30.
- Hales C.M., Carroll M.D., Fryar C.D., and Ogden C.L. 2017. “Prevalence of obesity among adults and youth: Unites States, 2015-2016.” NCHS data brief, no 288. Hyattsville, MD.
- Hanavan E.P. 1964. “A mathematical model of the human body.” Technical Report AMRL-TR-64-102, Aerospace Medical Research Laboratories, Wright-Patterson Air Force Base, Dayton, Ohio.
- Hangartner T.N. 2007. “A study of the long-term precision of dual-energy x-ray absorptiometry bone densitometers and implications for the validity of the least-significant-change calculations.” *Osteoporosis International* 18: 513-523.
- Hansen C., Venture G., Rezzoug N., Gorce P., and Isableu B. 2014. “An individual and dynamic body segment inertial parameter validation method using ground reaction forces.” *Journal of Biomechanics* 47: 1577-1581.
- Hertz H.P. 2004. "The impact of obesity on work limitations and cardiovascular risk factors in the U.S. workforce." *Journal of Occupational and Environmental Medicine* 46: 1196-1203.
- Hinrichs R.N. 1990. “Adjustments to the segment center of mass proportions of Clauser et al. (1969).” *Journal of Biomechanics* 23(9): 949-951.
- Hoang K-L.H. and Mombaur K. 2015. “Adjustments to de Leva—anthropometric regression data for the changes in body proportions in elderly humans.” *Journal of Biomechanics* 48: 3732-3736.
- Hodgdon, J. A. and Beckett, M. B. 1984a. “Prediction of percent body fat for U.S. Navy men from body circumferences and height.” Naval Health Research Center Report No. 84-11. San Diego, CA.
- Hodgdon, J. A. and Beckett, M. B. 1984b. “Prediction of percent body fat for U.S. Navy women from body circumferences and height.” Naval Health Research Center Report No. 84-29. San Diego, CA.
- Hughes V.A., Roubenoff R., Wood M., Frontera W.R., Evans W.J., and Fiatarone Singh MA. 2004. "Anthropometric assessment of 10-y changes in body composition in the elderly." *American Journal of Clinical Nutrition* 80: 475-482.
- Ingrova P., Kralik M, and Bartova V. 2017. “Relationships between the hand grip strength and body composition in Czech and Slovak Students.” *Slovenska Antropologia* 20: 30-43.

- Jackson A.S., Janssen I., Sui X., Church T.S., and Blair S.N. 2012. "Longitudinal changes in body composition associated with healthy ageing: men, aged 20-96 years." *British Journal of Nutrition* 107: 1085-1091.
- Jackson A.S. and Pollock M.L. 1978. "Generalized equations for predicting body density of men." *British Journal of Nutrition* 40:497-504.
- Jackson A.S., Pollock M.L., and Ward A. 1980. "Generalized equations for predicting body density of women." *Medicine & Science in Sports & Exercise* 12:175-181.
- Jackson A.S., Stanforth P.R., Gagnon J., Rankinen T., Leon A.S., Rao D.C., Skinner J.S., Bouchard C., and Wilmore J.H. 2002. "The effect of sex, age and race on estimating body fat from body mass index: The Heritage Family Study." *International Journal of Obesity* 26: 789-796.
- Jensen R.K. 1978. "Estimation of the biomechanical properties of three body types using a photogrammetric method." *Journal of Biomechanics* 11: 349-358.
- Kuczmarski M.F., Kuczmarski R.J., and Najjar M. 2000. "Descriptive anthropometric reference data for older Americans." *Journal of the American Dietetic Association* 100: 59-66.
- Kwok T., Woo J., and Lau E. 2001. "Prediction of body fat by anthropometry in older Chinese people." *Obesity Research* 9:97-101.
- Lad U.P., Satyanarayana P., Shisode-Lad S, Siri C.C., and Kumari N.R. 2013. "A study on the correlation between the body mass index (BMI), the body fat percentage, the handgrip strength, and the handgrip endurance in underweight, normal weight, and overweight adolescents." *Journal of clinical and Diagnostic Research* 7(1): 51-54.
- Lee C.M.Y., Huxley R.R., Wildman R.P., and Woodward M. 2008. "Indices of abdominal obesity are better discriminators of cardiovascular risk factors than BMI: A meta-analysis." *Journal of Clinical Epidemiology* 61: 646-653.
- Luckhaupt S.E., Cohen M.A., Li J., and Calvert G.M. 2014. "Prevalence of obesity among U.S. workers and associations with occupational factors." *American Journal of Preventative Medicine* 46(3): 237-248.
- Matrangola S.L., Madigan M.L., Nussbaum M.A., Ross R., and Davy K.P. 2008. "Changes in body segment inertial parameters of obese individuals with weight loss." *Journal of Biomechanics* 41: 3278-3281.
- McConville, J.T., Churchill, T.D., Kaleps, I., Clauser, C.E., and Cuzzi, J. 1980. Anthropometric relationships of body and body segment moments of inertia. Technical Report AFAMRL-TR-80-119, Aerospace Medical Research Laboratory, Wright-Patterson Air Force Base, Dayton, Ohio.

- Merrill Z., Bova G., Chambers A.J., and Cham R. 2018. "Effect of trunk segment boundary definitions on frontal plane segment inertia calculations." *Journal of Applied Biomechanics* 34(3) 232-235.
- Merrill Z., Chambers A.J., and Cham R. 2017. "Impact of age and body mass index on anthropometry in working adults." *Proceedings of the Human Factors and Ergonomics Society Annual Meeting* 61(1), 1341-1345.
- Miyatake N., Miyachi M., Tabata I., Sakano N., Hirao T., and Numata T. 2012. "Relationship between muscle strength and anthropometric, body composition parameters in Japanese adolescents." *Health* 4(1): 1-5.
- Morimoto A., Suga T., Tottori N., Wachi M., Misaki J., Tsuchikane R., and Isaka T. 2017. "Association between hand muscle thickness and whole-body skeletal muscle mass in healthy adults: A pilot study." *The Journal of Physical Therapy Science* 21: 1644-1648.
- Moyer B.E. 2006. "Slip and fall risks: Pre-slip gait contributions and post-slip response effects." Doctoral Dissertation, University of Pittsburgh.
- Myers A.H., Baker S.P., Li G., Smith G.S., Wilker S., Liang K.Y., and Johnson J.V. 1999. "Back injury in municipal workers: A case control study." *American Journal of Public Health* 89(7): 1036-1041.
- Ogden C.L., Carroll M.D., Fryar C.D., and Flegal K.M. 2015. "Prevalence of obesity among adults and youth: Unites States, 2011-2014." NCHS data brief, no 219. Hyattsville, MD.
- Ogden C.L., Carroll M.D., Kit B.K., and Flegal K.M. 2014. "Prevalence of childhood and adult obesity in the United States, 2011-2012." *Journal of the American Medical Association* 311(8): 806-814.
- Ortega F.B., Sue X., Lavie C.J., and Blair S.N. 2016. "Body mass index, the most widely used but also widely criticized index: Would a criterion measure of total body fat be a better predictor of cardiovascular mortality?" *Mayo Clinic Proceedings* 91(4): 443-455.
- Padwal R., Leslie W.D., Lix L.M., and Majumdar S.R. 2016. "Relationship among body fat percentage, body mass index, and all-cause mortality." *Annals of Internal Medicine* 164: 532-541.
- Park B.K. and Reed M.P. 2015. "Parametric body shape model of standing children aged 3-11 years." *Ergonomics* 58(10): 1714-1725.
- Pavol M.J., Owings T.M., and Grabiner M.D. 2002. "Body segment inertial parameter estimation for the general population of older adults." *Journal of Biomechanics* 35: 707-712.
- Pearsall D.J. and Costigan P.A. 1999. "The effect of segment parameter error on gait analysis results." *Gait & Posture* 9: 173-183.

- Pollack K.M. and Cheskin L.J. 2007. "Obesity and workplace traumatic injury: Does the science support the link?" *Injury Prevention* 13: 297-302.
- Rajae M.A., Arjmand N., Shirazi-Ali A., Plamondon A., and Schmidt H. 2015. "Comparative evaluation of six quantitative lifting tools to estimate spine loads during static activities." *Applied Ergonomics* 48: 22-32.
- Rao G., Amarantini D., Berton E., and Favier D. 2006. "Influence of body segments' parameters estimation models on inverse dynamics solutions during gait." *Journal of Biomechanics* 39: 1531-1536.
- Reed, M.P. and Ebert, S.M. 2013. "The Seated Soldier Study: Posture and Body Shape in Vehicle Seats." Technical Report UMTRI-2013-13. University of Michigan Transportation Research Institute, Ann Arbor, Michigan, USA.
- Russell S.J., Winnemuller L., Camp J.E., and Johnson P.W. 2007. "Comparing the results of five lifting analysis tools." *Applied Ergonomics* 38: 91-97.
- Sanders R.H., Chiu C-Y., Gonjo T., Thow J., Oliviera N., Psycharakis S.G., Payton C.J., and McCabe C.B. 2015. "Reliability of the elliptical zone method of estimating body segment parameters of swimmers." *Journal of Sports Science and Medicine* 14: 215-224.
- Shan G., and Bohn C. 2003. "Anthropometrical data and coefficients of regression related to gender and race." *Applied Ergonomics* 34: 327-337.
- Siri W.E. 1961. "Body composition from fluid spaces and density: analysis of methods." *Nutrition* 1993(9):480-491.
- St-Onge, M-P. 2005. "Relationship between body composition changes and changes in physical function and metabolic risk factors in aging." *Current Opinion in Clinical Nutrition and Metabolic Care* 8: 523-528.
- University of Michigan Center for Ergonomics – 3DSSPP. 2017. 3DStaticStrength Prediction Program User's Manual.
- Van Domelen D.R., Koster A., Caserotti P., Brychta R.J., Chen K.Y., McClain J.J., Troiano R.P., Berrigan D.A., and Harris T.B. 2011. "Employment and physical activity in the U.S." *American Journal of Preventative Medicine* 41(2): 136-145.
- Venture G., Ayusawa K., and Nakamura Y. 2009. "Real-time identification and visualization of human segment parameters." *Proceedings of the IEEE International Conference on Engineering in Medicine and Biology Society*, 3983-3986.
- Visser M., van den Heuvel E., and Deurenberg P. 1994. "Prediction equations for the estimation of body composition in the elderly using anthropometric data." *British Journal of Nutrition* 71(6): 823-833.

- Wicke J. and Dumas G.A. 2010. "Influence of the volume and density functions within geometric models for estimating trunk inertial parameters." *Journal of Applied Biomechanics* 26: 26-31.
- Woolcott O.O. and Bergman R.N. 2018. "Relative fat mass (RFM) as a new estimator of whole-body fat percentage—A cross-sectional study in American adult individuals." *Scientific Reports* 8: 10980.
- World Health Organization. "Waist circumference and waist-hip ratio: Report of a WHO expert consultation." Geneva: World Health Organization, 2008.
- Young, J.W., Chandler, R.F., Snow, C.C., Robinette, K.M., Zehner, G.F., and Lofberg, M.S. 1983. "Anthropometric and mass distribution characteristics of the adults female." Technical Report FA-AM-83-16, FAA Civil Aeromedical Institute, Oklahoma City, Oklahoma.